ISSN 1949-8470 (online)

World Journal of *Radiology*

World J Radiol 2011 September 28; 3(9): 215-240

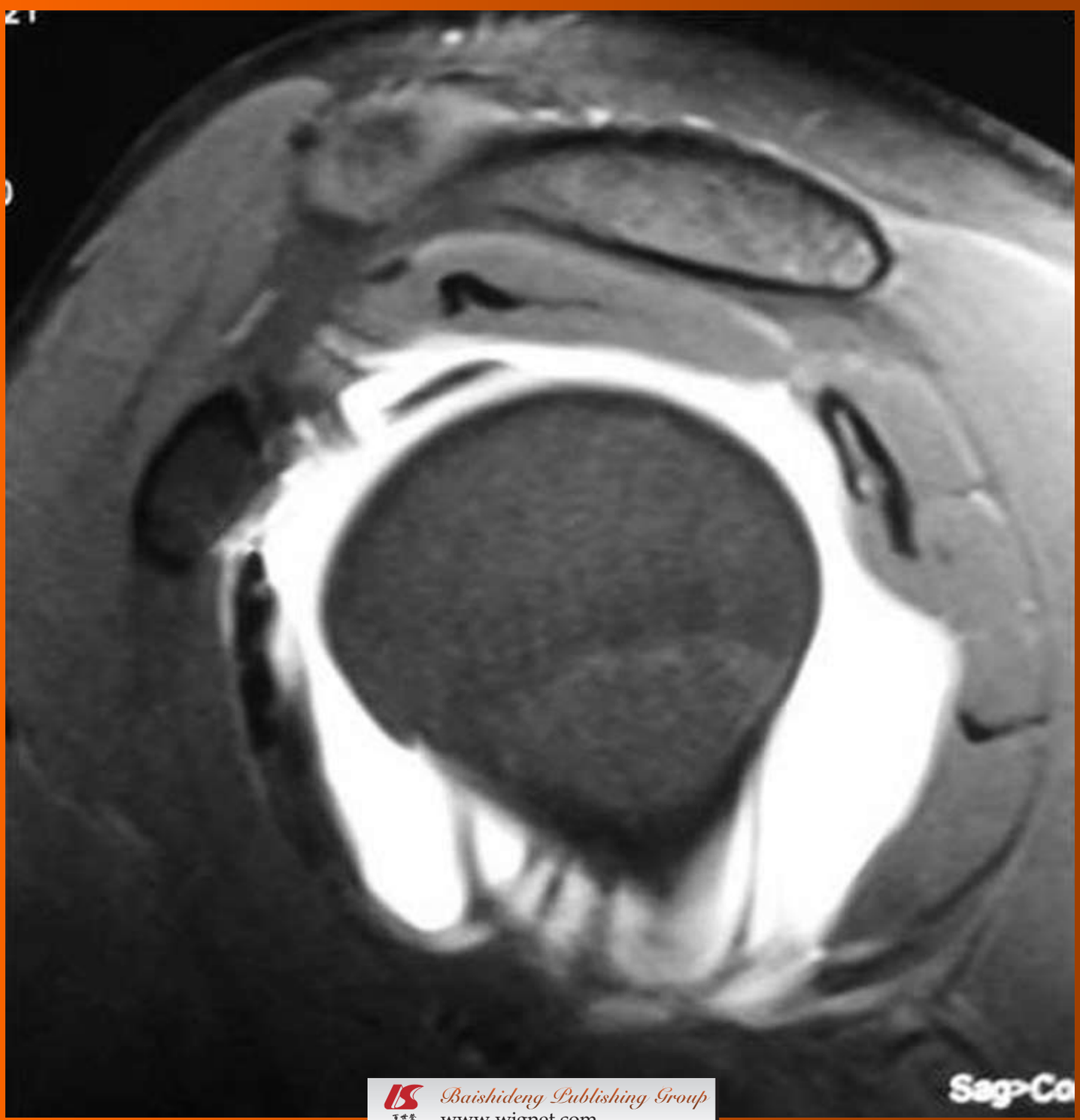

Baishideng Publishing Group
www.wjgnet.com

WJR World Journal of Radiology

A peer-reviewed, online, open-access journal of Radiology

Editorial Board

2009-2013

The *World Journal of Radiology* Editorial Board consists of 319 members, representing a team of worldwide experts in radiology. They are from 40 countries, including Australia (3), Austria (4), Belgium (5), Brazil (3), Canada (9), Chile (1), China (25), Czech (1), Denmark (1), Egypt (4), Estonia (1), Finland (1), France (6), Germany (17), Greece (8), Hungary (1), India (9), Iran (5), Ireland (1), Israel (4), Italy (28), Japan (14), Lebanon (1), Libya (1), Malaysia (2), Mexico (1), Netherlands (4), New Zealand (1), Norway (1), Saudi Arabia (3), Serbia (1), Singapore (2), Slovakia (1), South Korea (16), Spain (8), Switzerland (5), Thailand (1), Turkey (20), United Kingdom (16), and United States (82).

France

Alain Chapel, *Fontenay-Aux-Roses*
Nathalie Lassau, *Villejuif*
Youlia M Kirova, *Paris*
Géraldine Le Duc, *Grenoble Cedex*
Laurent Pierot, *Reims*
Frank Pilleul, *Lyon*
Pascal Pommier, *Lyon*

Germany

Ambros J Beer, *München*
Thomas Deserno, *Aachen*
Frederik L Giesel, *Heidelberg*
Ulf Jensen, *Kiel*
Markus Sebastian Juchems, *Ulm*
Kai U Juergens, *Bremen*
Melanie Kettering, *Jena*
Jennifer Linn, *Munich*
Christian Lohrmann, *Freiburg*
David Maintz, *Münster*
Henrik J Michaely, *Mannheim*
Oliver Micke, *Bielefeld*
Thoralf Niendorf, *Berlin-Buch*
Silvia Obenauer, *Duesseldorf*
Steffen Rickes, *Halberstadt*
Lars V Baron von Engelhardt, *Bochum*
Goetz H Welsch, *Erlangen*

Greece

Panagiotis Antoniou, *Alexandroupolis*
George C Kagadis, *Rion*
Dimitris Karacostas, *Thessaloniki*
George Panayiotakis, *Patras*
Alexander D Rapidis, *Athens*
C Triantopoulou, *Athens*
Ioannis Tsalafoutas, *Athens*
Virginia Tsapaki, *Anixi*
Ioannis Valais, *Athens*

Hungary

Peter Laszlo Lakatos, *Budapest*

India

Anil Kumar Anand, *New Delhi*
Surendra Babu, *Tamilnadu*
Sandip Basu, *Bombay*
Kundan Singh Chufal, *New Delhi*
Shivanand Gamanagatti, *New Delhi*
Vimoj J Nair, *Haryana*
R Prabhakar, *New Delhi*
Sanjeeb Kumar Sahoo, *Orissa*

Iran

Vahid Reza Dabbagh Kakhki, *Mashhad*
Mehran Karimi, *Shiraz*
Farideh Nejat, *Tehran*
Alireza Shirazi, *Tehran*
Hadi Rokni Yazdi, *Tehran*

Ireland

Joseph Simon Butler, *Dublin*

Israel

Amit Gefen, *Tel Aviv*
Eyal Sheiner, *Be'er-Sheva*
Jacob Sosna, *Jerusalem*
Simcha Yagel, *Jerusalem*

Italy

Mohssen Ansarin, *Milan*
Stefano Arcangeli, *Rome*
Tommaso Bartalena, *Imola*
Filippo Cademartiri, *Parma*
Sergio Casciaro, *Lecce*
Laura Crocetti, *Pisa*
Alberto Cuocolo, *Napoli*
Mirko D'Onofrio, *Verona*
Massimo Filippi, *Milan*
Claudio Fiorino, *Milano*
Alessandro Franchello, *Turin*
Roberto Grassi, *Naples*
Stefano Guerriero, *Cagliari*
Francesco Lassandro, *Napoli*
Nicola Limbucci, *L'Aquila*
Raffaele Lodi, *Bologna*
Francesca Maccioni, *Rome*
Laura Martincich, *Candiolo*
Mario Mascalchi, *Florence*
Roberto Miraglia, *Palermo*
Eugenio Picano, *Pisa*
Antonio Pinto, *Naples*
Stefania Romano, *Naples*
Luca Saba, *Cagliari*
Sergio Sartori, *Ferrara*
Mariano Scaglione, *Castel Volturno*
Lidia Strigari, *Rome*
Vincenzo Valentini, *Rome*

Japan

Shigeru Ehara, *Morioka*
Nobuyuki Hamada, *Chiba*
Takao Hiraki, *Okayama*
Akio Hiwatashi, *Fukuoka*
Masahiro Jinzaki, *Tokyo*
Hiroshi Matsuda, *Saitama*
Yasunori Minami, *Osaka*
Jun-Ichi Nishizawa, *Tokyo*
Tetsu Niwa, *Yokohama*
Kazushi Numata, *Kanagawa*
Kazuhiko Ogawa, *Okinawa*
Hitoshi Shibuya, *Tokyo*
Akira Uchino, *Saitama*
Haiquan Yang, *Kanagawa*

Lebanon

Aghiad Al-Kutoubi, *Beirut*

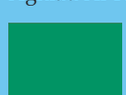

Libya

Anuj Mishra, *Tripoli*

Malaysia

R Logeswaran, *Cyberjaya*
Kwan-Hoong Ng, *Kuala Lumpur*

Mexico

Heriberto Medina-Franco, *Mexico City*

Netherlands

Jurgen J Fütterer, *Nijmegen*
Raffaella Rossin, *Eindhoven*
Paul E Sijens, *Groningen*
Willem Jan van Rooij, *Tilburg*

New Zealand

W Howell Round, *Hamilton*

Norway

Arne Sigmund Borthne, *Lørenskog*

Saudi Arabia

Mohammed Al-Omran, *Riyadh*
Ragab Hani Donkol, *Abha*
Volker Rudat, *Al Khobar*

Serbia

Djordjije Saranovic, *Belgrade*

Singapore

Uei Pua, *Singapore*
Lim CC Tchoyoson, *Singapore*

Slovakia

František Dubecký, *Bratislava*

South Korea

Bo-Young Choe, *Seoul*
Joon Koo Han, *Seoul*
Seung Jae Huh, *Seoul*
Chan Kyo Kim, *Seoul*
Myeong-Jin Kim, *Seoul*
Seung Hyup Kim, *Seoul*
Kyoung Ho Lee, *Gyeonggi-do*
Won-Jin Moon, *Seoul*
Wazir Muhammad, *Daegu*
Jai Soung Park, *Bucheon*
Noh Hyuck Park, *Kyunggi*
Sang-Hyun Park, *Daejeon*
Joon Beom Seo, *Seoul*
Ji-Hoon Shin, *Seoul*
Jin-Suck Suh, *Seoul*
Hong-Gyun Wu, *Seoul*

Spain

Eduardo J Aguilar, *Valencia*
Miguel Alcaraz, *Murcia*
Juan Luis Alcazar, *Pamplona*
Gorka Bastarrika, *Pamplona*
Rafael Martínez-Monge, *Pamplona*
Alberto Muñoz, *Madrid*
Joan C Vilanova, *Girona*

Switzerland

Nicolau Beckmann, *Basel*
Silke Grabherr, *Lausanne*
Karl-Olof Lövblad, *Geneva*
Tilo Niemann, *Basel*
Martin A Walter, *Basel*

Thailand

Sudsriluk Sampatchalit, *Bangkok*

Turkey

Olus Api, *Istanbul*
Kubilay Aydin, *İstanbul*
Işıl Bilgen, *Izmir*
Zulkif Bozgeyik, *Elazig*
Barbaros E Çil, *Ankara*
Gulgun Engin, *Istanbul*
M Fatih Evcimik, *Malatya*
Ahmet Kaan Gündüz, *Ankara*
Tayfun Hakan, *Istanbul*
Adnan Kabaalioglu, *Antalya*
Fehmi Kaçmaz, *Ankara*
Musturay Karcaaltincaba, *Ankara*
Osman Kizilkilic, *Istanbul*
Zafer Koc, *Adana*
Cem Onal, *Adana*
Yahya Paksoy, *Konya*
Bunyamin Sahin, *Samsun*
Ercument Unlu, *Edirne*
Ahmet Tuncay Turgut, *Ankara*
Ender Uysal, *Istanbul*

United Kingdom

K Faulkner, *Wallsend*
Peter Gaines, *Sheffield*
Balaji Ganeshan, *Brighton*
Nagy Habib, *London*
Alan Jackson, *Manchester*
Pradesh Kumar, *Portsmouth*
Tarik F Massoud, *Cambridge*
Igor Meglinski, *Bedfordshire*
Robert Morgan, *London*
Ian Negus, *Bristol*
Georgios A Plataniotis, *Aberdeen*
N J Raine-Fenning, *Nottingham*
Manuchehr Soleimani, *Bath*
MY Tseng, *Nottingham*
Edwin JR **van Beek,** *Edinburgh*
Feng Wu, *Oxford*

United States

Athanassios Argiris, *Pittsburgh*
Stephen R Baker, *Newark*
Lia Bartella, *New York*
Charles Bellows, *New Orleans*
Walter L Biffl, *Denver*
Homer S Black, *Houston*
Wessam Bou-Assaly, *Ann Arbor*
Owen Carmichael, *Davis*
Shelton D Caruthers, *St Louis*
Yuhchyau Chen, *Rochester*
Melvin E Clouse, *Boston*
Ezra Eddy Wyssam Cohen, *Chicago*
Aaron Cohen-Gadol, *Indianapolis*
Patrick M Colletti, *Los Angeles*
Kassa Darge, *Philadelphia*
Abhijit P Datir, *Miami*
Delia C DeBuc, *Miami*
Russell L Deter, *Houston*
Adam P Dicker, *Phil*
Khaled M Elsayes, *Ann Arbor*
Steven Feigenberg, *Baltimore*
Christopher G Filippi, *Burlington*
Victor Frenkel, *Bethesda*
Thomas J **George Jr,** *Gainesville*
Patrick K Ha, *Baltimore*
Robert I Haddad, *Boston*
Walter A Hall, *Syracuse*
Mary S Hammes, *Chicago*
John Hart Jr, *Dallas*
Randall T Higashida, *San Francisco*
Juebin Huang, *Jackson*
Andrei Iagaru, *Stanford*
Craig Johnson, *Milwaukee*
Ella F Jones, *San Francisco*
Csaba Juhasz, *Detroit*
Riyad Karmy-Jones, *Vancouver*
Daniel J **Kelley,** *Madison*
Amir Khan, *Longview*
Euishin Edmund Kim, *Houston*
Vikas Kundra, *Houston*
Kennith F Layton, *Dallas*
Rui Liao, *Princeton*
CM Charlie Ma, *Philadelphia*
Nina A Mayr, *Columbus*
Thomas J Meade, *Evanston*
Steven R **Messé,** *Philadelphia*
Nathan Olivier Mewton, *Baltimore*
Feroze B Mohamed, *Philadelphia*
Koenraad J Mortele, *Boston*
Mohan Natarajan, *San Antonio*
John L Nosher, *New Brunswick*
Chong-Xian Pan, *Sacramento*
Dipanjan Pan, *St Louis*
Martin R Prince, *New York*
Reza Rahbar, *Boston*
Carlos S Restrepo, *San Antonio*
Veronica Rooks, *Honolulu*
Maythem Saeed, *San Francisco*
Edgar A Samaniego, *Palo Alto*
Kohkan Shamsi, *Doylestown*
Jason P Sheehan, *Charlottesville*
William P Sheehan, *Willmar*
Charles Jeffrey Smith, *Columbia*
Monvadi B Srichai-Parsia, *New York*
Dan Stoianovici, *Baltimore*
Janio Szklaruk, *Houston*
Dian Wang, *Milwaukee*
Jian Z Wang, *Columbus*
Liang Wang, *New York*
Shougang Wang, *Santa Clara*
Wenbao Wang, *New York*
Aaron H Wolfson, *Miami*
Gayle E Woloschak, *Chicago*
Ying Xiao, *Philadelphia*
Juan Xu, *Pittsburgh*
Benjamin M Yeh, *San Francisco*
Terry T Yoshizumi, *Durham*
Jinxing Yu, *Richmond*
Jianhui Zhong, *Rochester*

WJR World Journal of Radiology

Contents

Monthly Volume 3 Number 9 September 28, 2011

World Journal of Radiology
Volume 3 Number 9 September 28, 2011

Contents

NAME OF JOURNAL
World Journal of Radiology

LAUNCH DATE
December 31, 2009

SPONSOR
Beijing Baishideng BioMed Scientific Co., Ltd.,
Room 903, Building D, Ocean International Center,
No. 62 Dongsihuan Zhonglu, Chaoyang District,
Beijing 100025, China
Telephone: +86-10-8538-1892
Fax: +86-10-8538-1893
E-mail: baishideng@wjgnet.com
http://www.wjgnet.com

EDITING
Editorial Board of *World Journal of Radiology*,
Room 903, Building D, Ocean International Center,
No. 62 Dongsihuan Zhonglu, Chaoyang District,
Beijing 100025, China
Telephone: +86-10-8538-1892
Fax: +86-10-8538-1893
E-mail: wjr@wjgnet.com
http://www.wjgnet.com

PUBLISHING
Baishideng Publishing Group Co., Limited,
Room 1701, 17/F, Henan Building,
No.90 Jaffe Road, Wanchai, Hong Kong, China
Fax: +852-3115-8812
Telephone: +852-5804-2046

E-mail: baishideng@wjgnet.com
http://www.wjgnet.com

SUBSCRIPTION
Beijing Baishideng BioMed Scientific Co., Ltd.,
Room 903, Building D, Ocean International Center,
No. 62 Dongsihuan Zhonglu, Chaoyang District,
Beijing 100025, China
Telephone: +86-10-8538-1892
Fax: +86-10-8538-1893
E-mail: baishideng@wjgnet.com
http://www.wjgnet.com

PUBLICATION DATE
September 28, 2011

ISSN
ISSN 1949-8470 (online)

EDITORIAL OFFICE
Na Ma, Director
World Journal of Radiology
Room 903, Building D, Ocean International Center,
No. 62 Dongsihuan Zhonglu, Chaoyang District,
Beijing 100025, China
Telephone: +86-10-8538-1892
Fax: +86-10-8538-1893
E-mail: wjr@wjgnet.com
http://www.wjgnet.com

INSTRUCTIONS TO AUTHORS
Full instructions are available online at http://www.wjgnet.com/1949-8470/g_info_20100316162358.htm.

ONLINE SUBMISSION
http://www.wjgnet.com/1949-8470office

World Journal of Radiology

Online Submissions: http://www.wjgnet.com/1949-8470office
wjr@wjgnet.com
doi:10.4329/wjr.v3.i9.215

World J Radiol 2011 September 28; 3(9): 215-223
ISSN 1949-8470 (online)

EDITORIAL

MDCT, MR and interventional radiology in biliary atresia candidates for liver transplantation

Roberto Miraglia, Settimo Caruso, Luigi Maruzzelli, Marco Spada, Silvia Riva, Marco Sciveres, Angelo Luca

Roberto Miraglia, Settimo Caruso, Luigi Maruzzelli, Angelo Luca, Department of Diagnostic and Interventional Radiology, Mediterranean Institute for Transplantation and Advanced Specialized Therapies, University of Pittsburgh Medical Center, 90127 Palermo, Italy
Marco Spada, Department of Transplantation Surgery, Mediterranean Institute for Transplantation and Advanced Specialized Therapies, University of Pittsburgh Medical Center, 90127 Palermo, Italy
Silvia Riva, Marco Sciveres, Department of Pediatric Hepatology, Mediterranean Institute for Transplantation and Advanced Specialized Therapies, University of Pittsburgh Medical Center, 90127 Palermo, Italy
Author contributions: Miraglia R wrote the paper and performed interventional radiology procedures; Caruso S and Maruzzelli L performed literature research and diagnostic and interventional radiology procedures; Spada M, Riva S and Sciveres M performed patients' surgical and clinical management; Luca A performed interventional radiology procedures and reviewed the final version of the paper.
Correspondence to: Roberto Miraglia, MD, Department of Diagnostic and Interventional Radiology, Mediterranean Institute for Transplantation and Advanced Specialized Therapies, Via Tricomi 1, 90127 Palermo, Italy. rmiraglia@ismett.edu
Telephone: +39-091-2192111 Fax: +39-091-2192344
Received: March 2, 2011 Revised: July 18, 2011
Accepted: July 25, 2011
Published online: September 28, 2011

Abstract

The multi-detector computed tomography (MDCT) scan and magnetic resonance (MR) of the abdomen play a key role in the work-up to liver transplantation (LT) by identifying congenital anomalies or cirrhosis-related modifications, conditions that can require changes in surgical technique. Moreover, the MDCT and MR scans allow identification of cirrhotic liver hepatic masses, extrahepatic porto-systemic shunts, eventual thrombosis of portal system and radiological signs of portal hypertension associated with biliary atresia (BA). The aim of this paper is to review MDCT, MR imaging and interventional radiology procedures performed to evaluate morphological changes and degree of portal hypertension in pediatric patients with end-stage liver disease secondary to BA, who are candidates for LT. Advances in the field of MR, MDCT and in percutaneous minimally invasive techniques have increased the importance of radiology in the management of pediatric patients with BA who are candidates for LT.

Key words: Portal hypertension; Imaging; Children; Cholangiopathy; Transplant

Peer reviewer: Frank Pilleul, MD, PhD, Professor, Department of Radiology, Hospices Civils de Lyon, CHU E. Herriot, Pavillon H, Department of Gastrointestinal Imaging, Place d'Arsonval, 69003 Lyon, Cedex, France

Miraglia R, Caruso S, Maruzzelli L, Spada M, Riva S, Sciveres M, Luca A. MDCT, MR and interventional radiology in biliary atresia candidates for liver transplantation *World J Radiol* 2011; 3(9): 215-223 Available from: URL: http://www.wjgnet.com/1949-8470/full/v3/i9/215.htm DOI: http://dx.doi.org/10.4329/wjr.v3.i9.215

INTRODUCTION

Biliary atresia (BA) is a neonatal cholangiopathy of unknown pathogenesis characterized by fibrosclerosis and obliteration of the biliary ducts which leads to cholestasis, progressive fibrosis and ultimately cirrhosis and death if untreated. The condition appears after birth with jaundice. Diagnosis is usually suspected on ultrasound[1,2], hepatobiliary scintigraphy and liver biopsy and confirmed by surgical cholangiography. Primary treatment of BA is the hepato-portoenterostomy (Kasai procedure) to reestablish bile flow, delaying fibrosis and biliary cirrhosis. The Kasai procedure, especially if performed before 2 mo of age, both reduces and delays the need for

liver transplantation (LT). However, the Kasai procedure is often not curative because liver function usually worsens progressively, leading to continuing cholangitis. LT, however, becomes the only therapeutic option in patients with long-standing BA.

BA represents the most common indication for LT in pediatric patients[3-5].

The multi-detector computed tomography (MDCT) scan and magnetic resonance (MR) of the abdomen play a key role in the work-up to LT by identifying congenital anomalies or cirrhosis-related modifications, conditions that can require changes in surgical technique. Moreover, the MDCT and MR scans allow identification of cirrhotic liver hepatic masses (often not easily identified with ultrasound in a cirrhotic liver), extrahepatic portosystemic shunts, eventual thrombosis of portal system and radiological signs of portal hypertension associated with BA[6-9].

The aim of this paper is to review multimodality diagnostic imaging and interventional radiology procedures performed to evaluate pediatric patients with end-stage liver disease secondary to BA who are candidates for LT.

PORTAL HYPERTENSION

Portal hypertension is an almost unavoidable consequence of BA with a wide variety of complications including ascites and bleeding from gastroesophageal varices, which represent the leading causes for LT and death in BA children with end-stage liver disease. The risk of death or need for LT after an initial episode of esophageal variceal hemorrhage in patients with BA is 50% at 6 years with a variable prognosis related to serum bilirubin concentration at the time of the episode[10]. In the long term, less then 18% of patients with BA, treated with corrective surgery, can avoid LT but require, in any case, assiduous lifelong care; in these patients clinical, ultrasound or endoscopic signs of portal hypertension are frequently present and gastrointestinal bleeding has been reported in 50% of cases, indicating that portal hypertension is also a major problem in patients in whom the Kasai procedure restores a sufficient bile flow[11].

While there are evidence-based approaches to the management of adults with portal hypertension, these are not available for children, hence making it difficult for pediatric hepatologists to determine whether recent advances in the management of portal hypertension in adults can be extrapolated to pediatric patients[12,13].

Portal pressure, in chronic liver diseases, is commonly measured by the hepatic venous pressure gradient (HVPG), defined as the difference between wedged (occluded) and free hepatic venous pressures with normal values ranging between 1-5 mmHg in adult patients. In adult patients with cirrhosis this measurement has been shown to be reproducible and the best predictor of the complications of portal hypertension[14-16]. It is well known that varices, variceal bleeding, portal hypertensive gastropathy and ascites do not occur until the HVPG increases above 10 mmHg, a pressure threshold defining clinically significant portal hypertension. Actually, although hepatic vein catheterization has been used in children undergoing TIPS procedure or transjugular liver biopsy[17,18], there are no reports of measurements of HVPG in pediatric series; there are no data regarding the normal values of portal pressure in healthy children, and no data regarding the use of HVPG in the evaluation of portal hypertension, nor in assessing response to therapy, although this has been recommended in international consensus conferences[12,13].

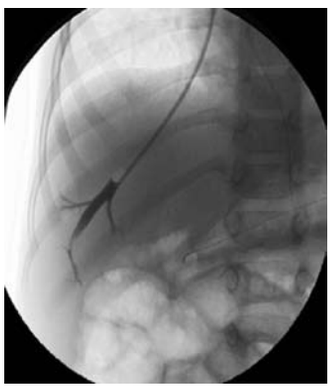

Figure 1 A 3-year-old male child post-Kasai. Fluoroscopic image of normal wedged venogram, hepatic venous pressure gradient 15.5 mmHg.

Our experience has showed HVPG to be a feasible and safe procedure in BA patients with advanced liver diseases and patent portal vein. The scenarios where HVPG may be useful in children with BA are the diagnosis of portal hypertension and the evaluation of the effects of preventive pharmacological therapy. In our experience, HVPG measurement in pediatric patients is performed after overnight fast in the angiographic suite under monitored anesthesia care with spontaneous respiration and local anesthesia, or under general anesthesia. The right internal jugular vein is punctured under ultrasound guidance. The hepatic vein, right or middle, is catheterized under fluoroscopic guidance with a 5F or 4F Cobra 2 angiographic catheter and a hydrophilic wire. The hepatic venogram is performed by hand with gentle injections of a small amount (2 to 6 cc) of iso-osmolar contrast medium with the catheter tip positioned in the mid/distal portion of the vein. The angiographic catheter is then exchanged with a standard 5F occlusion balloon catheter. Wedged (occluded) hepatic vein pressure (WHVP) and free hepatic vein pressure (FHVP) are obtained by inflating and releasing the balloon. The HVPG is estimated from the difference between WHPV and FHVP (Figure 1). Unexpectedly, intrahepatic venous-venous shunts (IVVS) are frequently detected in BA patients (Figure 2A). This is relevant with regards to the use of HVPG as a measurement of portal pressure. Obviously when the presence of IVVS precludes the total occlusion of the outflow from a hepatic vein, the pressure measured no longer equilibrates with the portal pressure, resulting in a gross underestimation of portal pressure as it occurs in patients with presi-

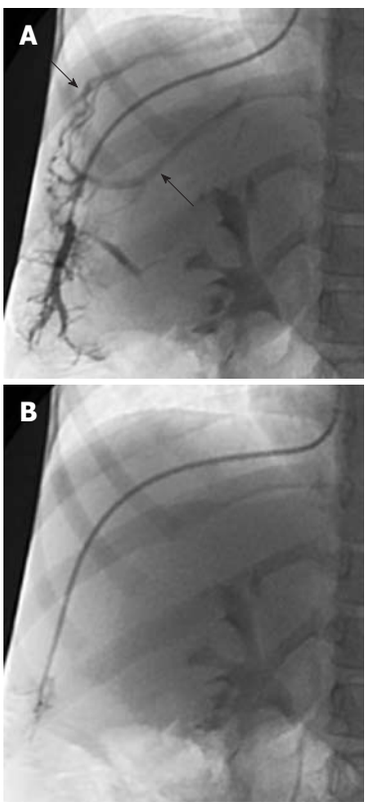

Figure 2 A 5-year-old female child post-Kasai. Fluoroscopic image. A: Wedged venogram showing multiple peripheral venovenous communications (arrows); B: 5F occlusion balloon catheter advanced distally in the hepatic vein, no venous communications visualized; Wedged (occluded) hepatic vein pressure obtained, hepatic venous pressure gradient 15 mmHg.

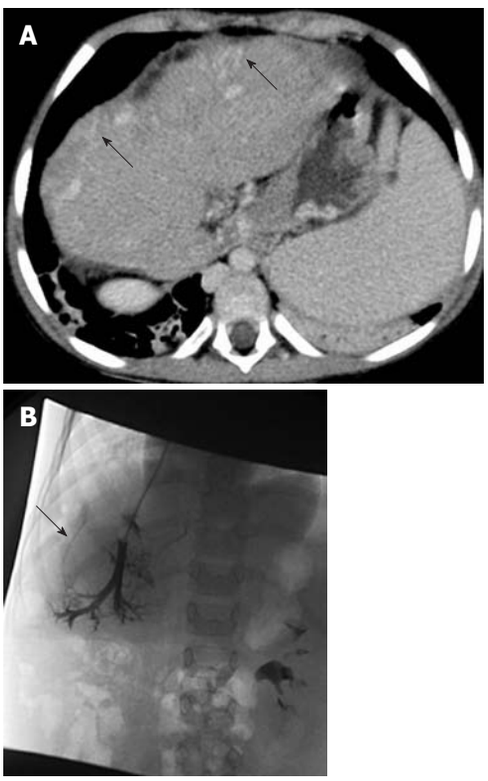

Figure 3 A 5-year-old female child post-Kasai. A: Multi-detector computed tomography shows peripheral venous-venous communications (arrows). Of note: Azygos vein dilatation secondary to retro-hepatic interruption of inferior vena cava; B: Fluoroscopic image: wedged venogram confirms peripheral venovenous communications (arrow).

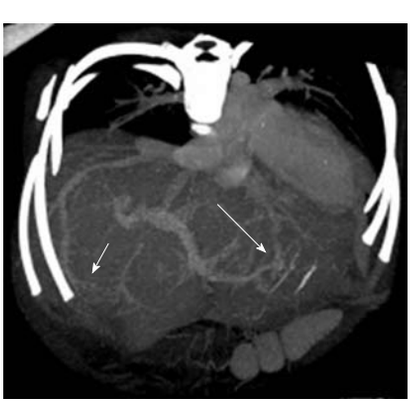

Figure 4 A 9-mo-old boy post-Kasai. Multi-detector computed tomography: Paraxial multi intensity projection reconstruction shows peripheral venous-venous communication (short arrow) and portal venous shunts (long arrow).

nusoidal intrahepatic portal hypertension. In our patients with BA and multiple IVVS, the WHVP had to be measured distally in the hepatic vein to avoid the shunt precluding an effective occlusion of the hepatic vein outflow, hence measuring the WHVP of a small vascular territory (Figure 2B). Veno-venous shunts are usually detected, with MDCT, in the portal-venous phase near the liver surface in the axial plane and can be confirmed in 3D reconstructions (Figures 3 and 4). BA patients frequently also show portal-venous shunts (Figure 4); only a few cases of communication between the portal and hepatic venous systems have been described in pediatric patients[19-21].

Because the severity and progression of portal hypertension influence the timing of LT, MDCT and MR imaging of portal hypertension (gastro-esophageal varices, perisplenic-perigastric varices, spontaneous spleno-renal shunt, ascites, splenomegaly), as an adjunct to endoscopic and clinical evaluations, have acquired an important role in patient follow-up.

VASCULAR ANOMALIES

In BA patients, anatomical variants of the hepatic artery, portal vein hypoplasia or thrombosis of the main portal vein (MPV) can require changes of surgical technique. Thus, preoperative depiction of any vascular anomalies offers the possibility of precise surgical planning reducing the risk of operative and postoperative complications.

For the very good morphologic and vascular imaging that can determine changes in surgical planning, MDCT is considered, in our hospital, the most important diagnostic tool in pediatric LT work-up. Compared with MR, MDCT offers the advantage of a better spatial and contrast resolution with a short examination time and consequently less time with the patient under sedation.

Radiation exposure is a relative disadvantage of MDCT; for this reason the use of pediatric parameters tailored on an individual basis is mandatory for maximal dose reduction obtaining satisfactory diagnostic images. Also, the need for intravenous iodinated contrast media is a relative disadvantage of MDCT although the occurrence of significant adverse effects in children is very rare[22]. In our experience, all the anatomical arterial variants and/or portal vein thrombosis or hypoplastic MPV cases were confirmed in the transplanted patients, confirming the high accuracy of the technique.

HEPATIC ARTERY

Anatomic and pathologic variation of the liver vasculature are frequent in BA patients[8,23]. In our experience, anatomical variants of the hepatic artery were found in 46% of cases (Figures 5 and 6); the most common variant was the common hepatic artery from the superior mesenteric artery. We also detected early bifurcation, right hepatic artery from the superior mesenteric artery, left hepatic artery from the left gastric artery, celiac-mesenteric common trunk, gastro-duodenal artery from segment 4 artery, accessory right hepatic artery from common hepatic artery, and left hepatic artery from the celiac artery. Occasionally, hepatic artery with intimal dissection or occluded hepatic artery have been reported in BA patients, which may be due to recurrent cholangitis or result from intraoperative injuries during Kasai procedures[7].

Hepatic artery variants can be easily managed by experienced surgeons in whole liver deceased donor LT because of the sufficient length of the graft hepatic artery for the anastomosis; however, a short hepatic artery can be a problem in partial LT, living related or from deceased donor.

The arterial axis of the graft usually includes the proper and common hepatic artery, in continuity with the celiac artery, and a patch of the aorta. The level of the anastomosis is chosen at any place along the recipient' s arterial axis, and the two vessels are trimmed to obtain a similar section and an adequate length. An end-to-end anastomosis is usually performed. If the recipient's arterial axis is deemed inadequate, the aorta can be clamped at the origin of the celiac artery or just below the renal arteries, and an end-to-side anastomosis can be performed at one of these sites. In the latter case, the interposition of an arterial graft from the donor, usually represented by an iliac artery, may be necessary. For those reasons a correct recipient hepatic artery evaluation is considered mandatory.

Frequently, BA patients show enlargement of the hepatic artery[1,2,7,24,25]. In a study performed in BA patients, at the diagnosis, mean hepatic artery diameter was 2.2 mm ± 0.59 mm[1]. Interestingly enough, in our experience, the mean diameter of the hepatic artery evaluated with MDCT in end-stage patients was 4.0 mm ± 1.2 mm[26]; this finding correlated well with the results of Humphrey *et al*[1] and could be the result of the hyperdynamic circulation secondary to cirrhotic changes of the liver, also reflecting, as a buffering effect, the reduction of portal flow in patients with thrombosis of the portal vein or the small portal vein.

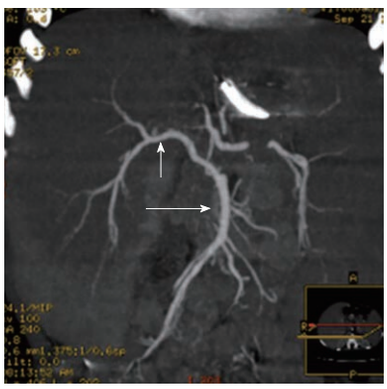

Figure 5 A 2-year-old female child post-Kasai. Multi-detector computed tomography: Multiple Intensity Projection reconstruction, right hepatic artery (short arrow) off from superior mesenteric artery (long arrow).

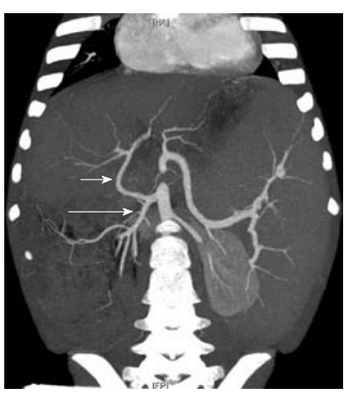

Figure 6 A 5-year-old female child post-Kasai. Multi-detector computed tomography: Multiple Intensity Projection reconstruction, common hepatic artery (short arrow) arising from superior mesenteric artery (long arrow). Of note: large splenomegaly.

PORTAL VEIN

Hypoplasia or thrombosis of the MPV in BA recipients can require changes of surgical technique during LT. Portal vein anastomosis during LT is usually performed in an end-to-end fashion. If the portal vein is small and sclerotic, it has to be dissected proximally to the confluence of the splenic and superior mesenteric vein, dividing the coronary vein of the stomach. The portal vein anastomosis will then be performed by means of a donor interposition vein graft. Patients with BA show higher risk of portal vein thrombosis than other pediatric recipients of LT[27] and the portal vein diameter of small recipients is strongly linked to the risk of thrombosis[28]. For this reason, surgeons have to know exactly the anatomy of the portal vein before LT (Figures 7 and 8). In our experience, thrombosis of the MPV in BA patients has an incidence of 15% while small portal vein, defined as

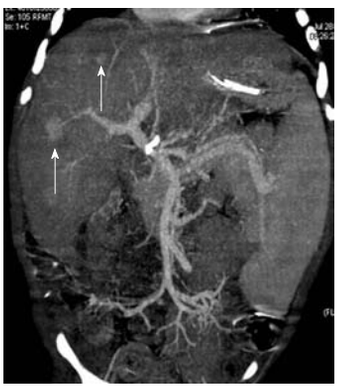

Figure 7 A 15-mo-old male child post-Kasai. Multi-detector computed tomography: Multiple Intensity Projection reconstruction. Good caliper of main portal vein, significant splenomegaly. Two hepatic hypervascular nodules coexist (arrows).

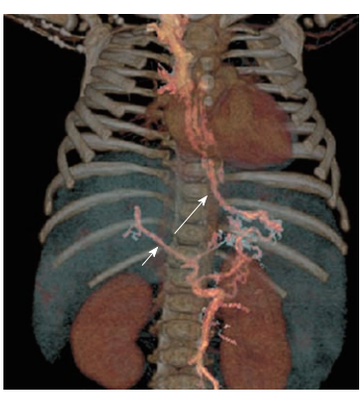

Figure 8 A 8-mo-old female child post-Kasai. Multi-detector computed tomography: volume rendering reconstruction shows small main portal vein (short arrow), patent coronary vein (long arrow) with filling of esophageal varices.

diameter of the MPV < 3 mm, has an incidence of 26%. Although rare, congenital absence of portal vein has also been reported in BA patients[29,30] (Figure 9).

VENA CAVA

Retro-hepatic interruption of the inferior vena cava, with azygeal continuation (Figure 3), is a rare vascular alteration described in BA patients, sometimes in association with polysplenia syndrome[9,31,32]. Although rare, its presence should be evaluated before LT because of possible complications regarding outflow reconstructions.

INTRAHEPATIC BILIARY CYSTS

Intrahepatic biliary cysts (IBC) are frequent in BA patients and reported in up to 30% of cases[33-37]. IBC are more frequent in post-Kasai patients. The mechanisms of cyst formation are unclear, although the extrahepatic as well as the intrahepatic duct fibro-obliterative process, inflammatory process and cirrhotic changes in the intralobular spaces are thought to be primary causes. Two types of IBC can be detected: solitary cysts (Figure 10A),

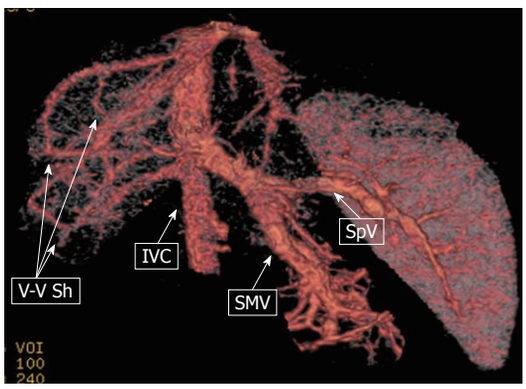

Figure 9 A 9-mo-old male child. Multi-detector computed tomography: volume rendering reconstruction shows the superior mesenteric vein (SMV) and the splenic vein (SpV) joining to form a short common trunk that directly enters into the suprarenal inferior vena cava (IVC); Venous-venous intrahepatic shunting (V-V Sh) coexist.

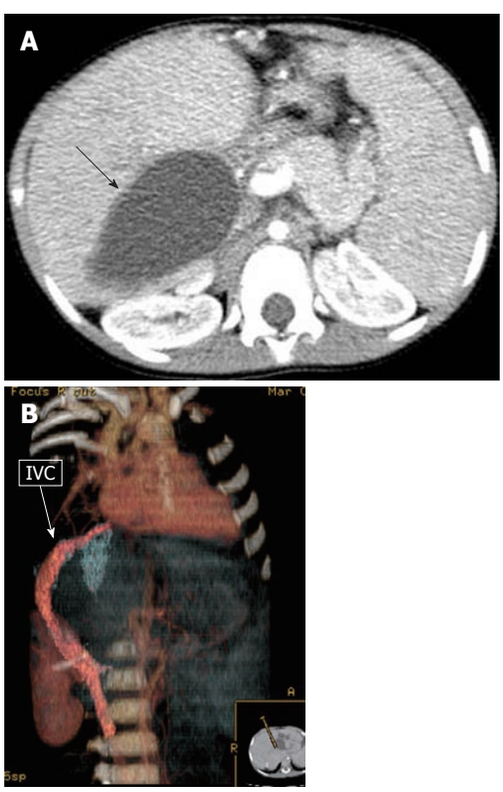

Figure 10 A 12-mo-old female child post-Kasai. A: Multi-detector computed tomography (MDCT), isolated large biliary cyst in the right lobe (arrow); B: MDCT, volume rendering reconstruction shows inferior vena cava (IVC) compressed and displaced by the large intrahepatic biliary cyst.

which are actually bile lakes, associated with poor prognosis[36] and likely determined by recurrent cholangitis; and continuous beaded cysts (Figures 11 and 12), which are dilated intrahepatic bile ducts and may be reversed. IBC are usually well detected with sonography. MDCT and MR both show good results in cyst detection and show advantages, compared to ultrasound, mainly in cases of large cysts as they can determine compression and/or dislodgment of vascular structures such as hepatic artery,

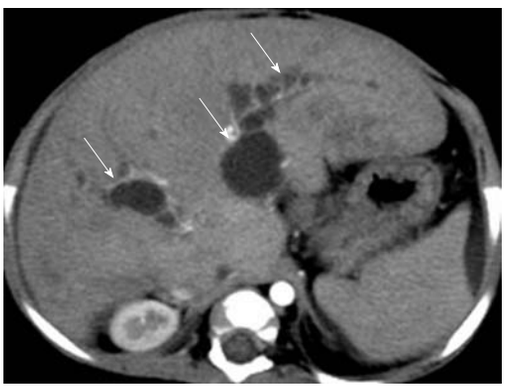

Figure 11 A 8-mo-old female child post-Kasai. Multi-detector computed tomography shows multiple intrahepatic biliary cysts after Kasai operation (arrows).

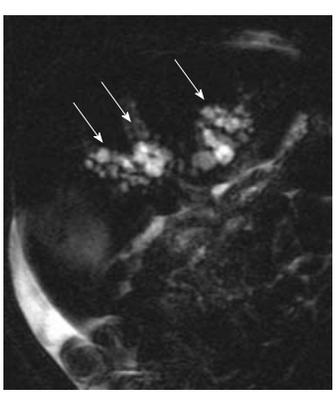

Figure 12 A 5-mo-old female child post-Kasai. Colangio magnetic resonance shows multiple intrahepatic biliary cysts (arrows).

portal vein and inferior vena cava (Figure 10B).

INTRAHEPATIC NODULES

Kasai surgery increases the survival of patients with BA[11]. The survival benefit of the Kasai procedure can delay subsequent LT, as primary LT in very young patients has a high morbidity and mortality rate. Postponing LT, however, leads to an increase in complication rate in the long-term survivor group having a native liver with evidence of various intrahepatic nodules. A pseudotumor, giant regenerative nodule, or macroregenerative nodule, like hepatocellular carcinoma, may be correlated with liver cirrhosis. Other tumors usually not associated with cirrhosis, such as focal nodular hyperplasia, regenerative nodular hyperplasia, hepatic cholangiocarcinoma and hepatic adenoma, have also been reported[3,38-46].

Lesion biopsy is considered the gold standard for the diagnosis of liver hepatic nodules, especially for hepatocellular carcinoma. However, this procedure has several limitations, including possible bleeding, a significant false negative rate, high interobserver variability in the differentiation between high-grade dysplastic nodules and well-differentiated hepatocellular carcinoma, as well as the possibility that the bioptic sample may not be representative of the entire lesion[39]. Furthermore, biopsy may not be technically possible because of lesion localization. In BA cirrhotic patients, liver biopsy may be contraindicated also because of the presence of ascites or impaired coagulation test and, most importantly, it is not uncommon to find that multiple hepatic nodules coexist in these patients. In this scenario, imaging with MR and/or MDCT plays a key role in liver nodule diagnosis of BA patients avoiding, when possible, liver biopsy. Although rare, hepatocellular carcinoma can occur in children with BA. In these patients serum α-fetoprotein level can be within normal range; for this reason there is the necessity for repeated sequential MR or MDCT imaging to monitor possible malignant transformation of liver nodules in patients with BA after Kasai operation. The prevalence of hepatocellular carcinoma in explanted livers of patients transplanted for BA has been reported to be 0.73%-2.44%[43-45]. Although the presence of hepatocellular carcinoma is not a contraindication to LT in BA patients, a delayed diagnosis can impair the post-transplant prognosis because node involvement, vascular invasion and tumor size are risk factors for recurrence of hepatocellular carcinoma after LT.

Imaging of hepatocellular carcinoma in children with BA has been reported as similar to hepatocellular carcinoma in adult patients with cirrhosis, with enhancement of the tumor in the arterial phase after contrast administration followed by hypointensity/hypodensity compared with the liver in the delayed phase indicating washout. Delayed enhancement of a fibrous tumor capsule and areas with intratumoral fatty infiltration has also been reported[41].

In our experience, we have not found hepatocellular carcinoma in BA patients before LT with MDCT and/or MR or at liver explants. Regenerative nodular hyperplasia nodules can be detected in BA patients. They are characterized by hyperplastic nodules composed of cells resembling normal hepatocytes. The nodules range in size from smaller than a hepatic acinus to conglomerate nodules forming large masses (Figure 13)[46]. Large nodules are hyperplastic lesions measuring between 5 mm and 5 cm in diameter that are larger than most cirrhotic nodules located in a liver that is otherwise abnormal[47,48]. Such lesions might be caused by an abnormal liver cell response to an altered portal flow. These benign nodules typically appear as iso-hyperintense in T1 images, isointense in T2 images, hypervascular on contrast-enhanced, cross-sectional imaging and have the potential to be misdiagnosed as hepatocellular carcinoma as they appear as hypervascular masses within a chronically diseased liver. Differently from hepatocellular carcinoma in portal venous and/or delayed phase, they have no washout. Regenerative nodular hyperplasia nodules have been described in association with congenital absence of portal vein[48] and also in Budd-Chiari syndrome. In Budd-Chiari patients, a 4% incidence of hepatocellular carcinoma has also been reported[49] and in several cases hepatocellular carcinoma showed no typical washout on portal venous phase. In

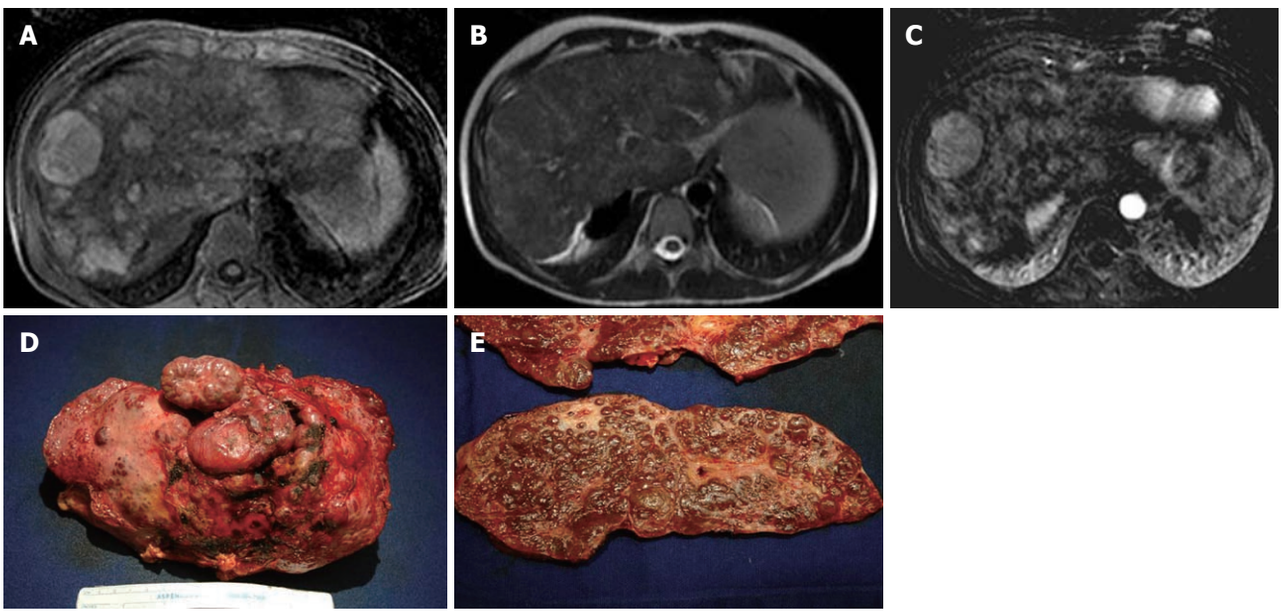

Figure 13 A 13-year-old male post-Kasai who underwent surgical spleno-renal shunt for gastrointestinal bleeding. A: Axial T1 Fat Sat weighted acquisition shows multiple hyperintense nodules, the largest of these in S8; B: Axial T2 weighted acquisition: the nodules are isointense; C: Axial T1 Fat Sat weighted acquisition obtained with digital subtraction between the arterial phase and the unenhanced phase shows the vascular enhancement of the nodules; D: Explanted liver shows an irregular and multilobulated surface; E: Gross examination of sectioned liver confirms the presence of multiple regenerative nodular hyperplasia nodules.

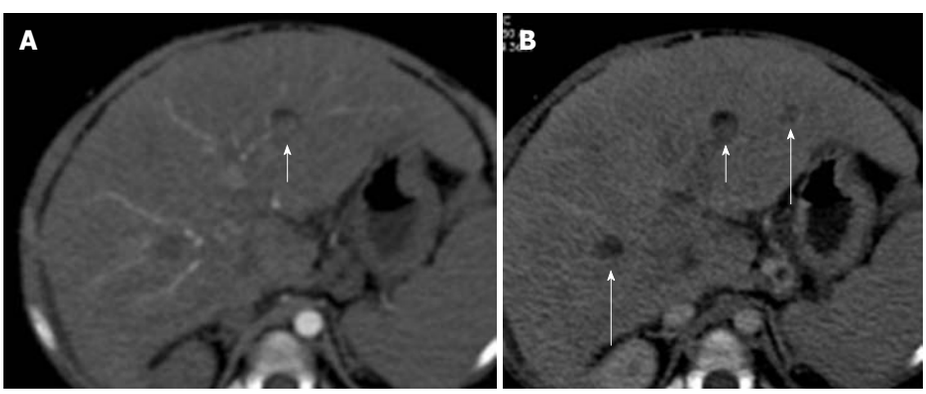

Figure 14 A 20-mo-old female without previous Kasai operation. Multi-detector computed tomography: In S3, nodule (short arrow) that shows in anterior portion a mild amount of fat. The nodule appears slightly hyperdense in arterial phase (A) and hypoattenuating in portal/venous phase; B: Regenerative nodule was found at liver explant. Of note: other hypoattenuating regenerative nodules in S6 and S3 (long arrows).

these patients increased α-fetoprotein level, increased size on successive imaging and the lack of a central scar were helpful for the diagnosis, although liver biopsy was performed to confirm hepatocellular carcinoma.

Macroregenerative nodule is occasionally encountered in BA cirrhotic livers[39,49]. A macroregenerative nodule is defined as a hepatocellular nodule containing one or more portal tracts located in a liver that is otherwise abnormal due to either cirrhosis or other severe disease[48]. These nodules typically appear as iso-hyperintense in T1 images and iso-hypointense in T2 images. The blood supply of a regenerative nodule comes largely from the portal vein, with minimal contribution from the hepatic artery. This vascular supply dynamic explains why there is no enhancement during the hepatic arterial phase on MR or MDCT images, with iso-hypointensity on portal venous-delayed phases (Figure 14).

In conclusion, we suggest following solid nodules with imaging in BA patients, proposing liver biopsy only for those with suspect morphological changes or in cases with increased α-fetoprotein level.

Advances in the field of MR, MDCT and in percutaneous minimally invasive techniques have increased the importance of radiology in the management of pediatric patients with BA who are candidates for LT.

REFERENCES

1 **Humphrey TM**, Stringer MD. Biliary atresia: US diagnosis. *Radiology* 2007; **244**: 845-851

2 **Lee MS**, Kim MJ, Lee MJ, Yoon CS, Han SJ, Oh JT, Park YN. Biliary atresia: color doppler US findings in neonates and infants. *Radiology* 2009; **252**: 282-289

3 **Liu YW**, Concejero AM, Chen CL, Cheng YF, Eng HL, Huang TL, Chen TY, Wang CC, Wang SH, Lin CC, Yong CC, Yang CH, Jordan AP, Jawan B. Hepatic pseudotumor in long-standing biliary atresia patients undergoing liver transplantation. *Liver Transpl* 2007; **13**: 1545-1551

4 **McKiernan PJ**, Baker AJ, Kelly DA. The frequency and outcome of biliary atresia in the UK and Ireland. *Lancet* 2000; **355**: 25-29

5 **McDiarmid SV**, Anand R, Lindblad AS. Studies of Pediatric Liver Transplantation: 2002 update. An overview of demographics, indications, timing, and immunosuppressive practices in pediatric liver transplantation in the United States and Canada. *Pediatr Transplant* 2004; **8**: 284-294

6 **Chen TY**, Chen CL, Huang TL, Chen YS, Wang CC, de Villa VH, Chiang YC, Jawan B, Cheng YF. Noninvasive multislice CT angiography in pediatric liver transplantation: a novel application. *Transplant Proc* 2003; **35**: 62-63

7 **Cheng YF**, Chen CL, Jawan B, Huang TL, Chen TY, Chen YS, Wang CC, de Villa V, Wang SH, Wah CK, Chiang YC, Eng HL, Lee TY, Goto S. Multislice computed tomography angiography in pediatric liver transplantation. *Transplantation* 2003; **76**: 353-357

8 **Tanano H**, Hasegawa T, Kawahara H, Sasaki T, Okada A. Biliary atresia associated with congenital structural anomalies. *J Pediatr Surg* 1999; **34**: 1687-1690

9 **Hasegawa T**, Kimura T, Sasaki T, Okada A. Living-related liver transplantation for biliary atresia associated with polysplenia syndrome. *Pediatr Transplant* 2002; **6**: 78-81

10 **Miga D**, Sokol RJ, Mackenzie T, Narkewicz MR, Smith D, Karrer FM. Survival after first esophageal variceal hemorrhage in patients with biliary atresia. *J Pediatr* 2001; **139**: 291-296

11 **Lykavieris P**, Chardot C, Sokhn M, Gauthier F, Valayer J, Bernard O. Outcome in adulthood of biliary atresia: a study of 63 patients who survived for over 20 years with their native liver. *Hepatology* 2005; **41**: 366-371

12 **de Franchis R**. Evolving consensus in portal hypertension. Report of the Baveno IV consensus workshop on methodology of diagnosis and therapy in portal hypertension. *J Hepatol* 2005; **43**: 167-176

13 **Shneider B**, Emre S, Groszmann R, Karani J, McKiernan P, Sarin S, Shashidhar H, Squires R, Superina R, de Ville de Goyet J, de Franchis R. Expert pediatric opinion on the Report of the Baveno IV consensus workshop on methodology of diagnosis and therapy in portal hypertension. *Pediatr Transplant* 2006; **10**: 893-907

14 **Groszmann RJ**, Wongcharatrawee S. The hepatic venous pressure gradient: anything worth doing should be done right. *Hepatology* 2004; **39**: 280-282

15 **D'Amico G**, Garcia-Pagan JC, Luca A, Bosch J. Hepatic vein pressure gradient reduction and prevention of variceal bleeding in cirrhosis: a systematic review. *Gastroenterology* 2006; **131**: 1611-1624

16 **Abraldes JG**, Tarantino I, Turnes J, Garcia-Pagan JC, Rodés J, Bosch J. Hemodynamic response to pharmacological treatment of portal hypertension and long-term prognosis of cirrhosis. *Hepatology* 2003; **37**: 902-908

17 **Habdank K**, Restrepo R, Ng V, Connolly BL, Temple MJ, Amaral J, Chait PG. Combined sonographic and fluoroscopic guidance during transjugular hepatic biopsies performed in children: a retrospective study of 74 biopsies. *AJR Am J Roentgenol* 2003; **180**: 1393-1398

18 **Johnson SP**, Leyendecker JR, Joseph FB, Joseph AE, Diffin DC, Devoid D, Eason J. Transjugular portosystemic shunts in pediatric patients awaiting liver transplantation. *Transplantation* 1996; **62**: 1178-1181

19 **Witters P**, Maleux G, George C, Delcroix M, Hoffman I, Gewillig M, Verslype C, Monbaliu D, Aerts R, Pirenne J, Van Steenbergen W, Nevens F, Fevery J, Cassiman D. Congenital veno-venous malformations of the liver: widely variable clinical presentations. *J Gastroenterol Hepatol* 2008; **23**: e390-e394

20 **Valls E**, Ceres L, Urbaneja A, Muñoz R, Alonso I. Color Doppler sonography in the diagnosis of neonatal intrahepatic portosystemic shunts. *J Clin Ultrasound* 2000; **28**: 42-46

21 **Yamagami T**, Nakamura T, Tokiwa K, Ohno K, Itoh H, Maeda T. Intrahepatic portosystemic venous shunt associated with biliary atresia: case report. *Pediatr Radiol* 2000; **30**: 489-491

22 **Dillman JR**, Strouse PJ, Ellis JH, Cohan RH, Jan SC. Incidence and severity of acute allergic-like reactions to i.v. nonionic iodinated contrast material in children. *AJR Am J Roentgenol* 2007; **188**: 1643-1647

23 **Yu CY**, Chen CL, Huang TL, Chen TY, Tsang LL, Ou HY, Concejero AM, Wang CC, Wang SH, Cheng YF. Preoperative imaging evaluation of the hepatic vasculature in biliary atresia patients undergoing LDLT: comparison of MDCT and MRI. *Pediatr Transplant* 2009; **13**: 984-989

24 **Kim WS**, Cheon JE, Youn BJ, Yoo SY, Kim WY, Kim IO, Yeon KM, Seo JK, Park KW. Hepatic arterial diameter measured with US: adjunct for US diagnosis of biliary atresia. *Radiology* 2007; **245**: 549-555

25 **dos Santos JL**, da Silveira TR, da Silva VD, Cerski CT, Wagner MB. Medial thickening of hepatic artery branches in biliary atresia. A morphometric study. *J Pediatr Surg* 2005; **40**: 637-642

26 **Caruso S**, Miraglia R, Milazzo M, Maruzzelli L, Pasta A, Spada M, Riva S, Luca A, Gridelli B. Multidetector computed tomography hepatic findings in children with end-stage biliary atresia. *Eur Radiol* 2010; **20**: 1468-1475

27 **Corno V**, Torri E, Bertani A, Guizzetti M, Lucianetti A, Maldini G, Pinelli D, Zambelli M, Aluffi A, Alberti D, Spada M, Gridelli B, Torre G, Colledan M. Early portal vein thrombosis after pediatric split liver transplantation with left lateral segment graft. *Transplant Proc* 2005; **37**: 1141-1142

28 **Chardot C**, Herrera JM, Debray D, Branchereau S, De Dreuzy O, Devictor D, Dartayet B, Norwood P, Lambert T, Pariente D, Gauthier F, Valayer J. Portal vein complications after liver transplantation for biliary atresia. *Liver Transpl Surg* 1997; **3**: 351-358

29 **Andreani P**, Srinivasan P, Ball CS, Heaton ND, Rela M. Congenital absence of the portal vein in liver transplantation for biliary atresia. *Int J Surg Investig* 2000; **2**: 81-84

30 **Taoube KA**, Alonso Calderón JL, Yandza T, St Vil D, Blanchard H. [Congenital absence of portal vein in a girl with biliary atresia treated with liver transplant]. *Cir Pediatr* 1999; **12**: 38-40

31 **Tarhan NC**, Ağildere AM, Boyvat F, Coşkun M, Ersoy H. Polysplenia syndrome with hepatic artery of superior mesenteric artery origin and a circumaortic renal vein. *Turk J Pediatr* 2000; **42**: 344-347

32 **Applegate KE**, Goske MJ, Pierce G, Murphy D. Situs revisited: imaging of the heterotaxy syndrome. *Radiographics* 1999; **19**: 837-852; discussion 853-854

33 **Takahashi A**, Tsuchida Y, Suzuki N, Kuroiwa M, Ikeda H, Hirato J, Hatakeyama S. Incidence of intrahepatic biliary cysts in biliary atresia after hepatic portoenterostomy and associated histopathologic findings in the liver and porta hepatis at diagnosis. *J Pediatr Surg* 1999; **34**: 1364-1368

34 **Takahashi A**, Tsuchida Y, Suzuki N, Kuroiwa M, Murai H, Toki F, Nomoto K, Kuwano H. Intrahepatic biliary cysts in biliary atresia in the era of liver transplantation. *J Pediatr Gastroenterol Nutr* 2003; **36**: 608-612

35 **Watanabe M**, Hori T, Kaneko M, Komuro H, Hirai M, Inoue S, Urita Y, Hoshino N. Intrahepatic biliary cysts in children with biliary atresia who have had a Kasai operation. *J Pediatr Surg* 2007; **42**: 1185-1189

36 **Tainaka T**, Kaneko K, Seo T, Ono Y, Sumida W, Ando H. Intrahepatic cystic lesions after hepatic portoenterostomy

for biliary atresia with bile lake and dilated bile ducts. *J Pediatr Gastroenterol Nutr* 2007; **44**: 104-107
37 **Tsuchida Y**, Honna T, Kawarasaki H. Cystic dilatation of the intrahepatic biliary system in biliary atresia after hepatic portoenterostomy. *J Pediatr Surg* 1994; **29**: 630-634
38 **Wang ZJ**, Coakley FV, Ferrell LD, Rosenthal P. CT and MRI of hepatic pseudotumor in long-standing biliary atresia. *J Comput Assist Tomogr* 2002; **26**: 444-447
39 **Stigliano R**, Burroughs AK. Should we biopsy each liver mass suspicious for HCC before liver transplantation?--no, please don't. *J Hepatol* 2005; **43**: 563-568
40 **Liang JL**, Cheng YF, Concejero AM, Huang TL, Chen TY, Tsang LL, Ou HY. Macro-regenerative nodules in biliary atresia: CT/MRI findings and their pathological relations. *World J Gastroenterol* 2008; **14**: 4529-4534
41 **Hol L**, van den Bos IC, Hussain SM, Zondervan PE, de Man RA. **Hepatocellular carcinoma complicating biliary atresia** after Kasai portoenterostomy. *Eur J Gastroenterol Hepatol* 2008; **20**: 227-231
42 **Sharp L**, Makin E, Davenport M. Hepatic haemangioendothelioma: a vertical association with biliary atresia? *Eur J Pediatr Surg* 2008; **18**: 277-279
43 **Tatekawa Y**, Asonuma K, Uemoto S, Inomata Y, Tanaka K. Liver transplantation for biliary atresia associated with malignant hepatic tumors. *J Pediatr Surg* 2001; **36**: 436-439
44 **Kohno M**, Kitatani H, Wada H, Kajimoto T, Matuno H, Tanino M, Nakagawa T, Takarada A. Hepatocellular carcinoma complicating biliary cirrhosis caused by biliary atresia: report of a case. *J Pediatr Surg* 1995; **30**: 1713-1716
45 **Esquivel CO**, Gutiérrez C, Cox KL, Garcia-Kennedy R, Berquist W, Concepcion W. Hepatocellular carcinoma and liver cell dysplasia in children with chronic liver disease. *J Pediatr Surg* 1994; **29**: 1465-1469
46 **Dachman AH**, Ros PR, Goodman ZD, Olmsted WW, Ishak KG. Nodular regenerative hyperplasia of the liver: clinical and radiologic observations. *AJR Am J Roentgenol* 1987; **148**: 717-722
47 **Okugawa Y**, Uchida K, Inoue M, Kawamoto A, Ohtake K, Sakurai H, Uchida K, Isaji S, Miki C, Kusunoki M. Focal nodular hyperplasia in biliary atresia patient after Kasai hepatic portoenterostomy. *Pediatr Surg Int* 2008; **24**: 609-612
48 **Grazioli L**, Alberti D, Olivetti L, Rigamonti W, Codazzi F, Matricardi L, Fugazzola C, Chiesa A. Congenital absence of portal vein with nodular regenerative hyperplasia of the liver. *Eur Radiol* 2000; **10**: 820-825
49 **Moucari R,** Rautou PE, Cazals-Hatem D, Geara A, Bureau C, Consigny Y, Francoz C, Denninger MH, Vilgrain V, Belghiti J, Durand F, Valla D, Plessier A. Hepatocellular carcinoma in Budd-Chiari syndrome: characteristics and risk factors. *Gut* 2008; **57:** 828-835

S- Editor Cheng JX **L- Editor** Logan S **E- Editor** Zheng XM

World Journal of Radiology

Online Submissions: http://www.wjgnet.com/1949-8470office
wjr@wjgnet.com
doi:10.4329/wjr.v3.i9.224

World J Radiol 2011 September 28; 3(9): 224-232
ISSN 1949-8470 (online)

REVIEW

Magnetic resonance imaging in glenohumeral instability

Manisha Jana, Shivanand Gamanagatti

Manisha Jana, Department of Radiodiagnosis, All India Institute of Medical Sciences, Ansari Nagar, 110029 New Delhi, India
Shivanand Gamanagatti, Department of Radiology, JPNA Trauma Centre, All India Institute of Medical Sciences, Ansari Nagar 110029 New Delhi, India
Author contributions: All authors have equally contributed to the manuscript drafting, manuscript revision and final manuscript checking.
Correspondence to: Dr. Shivanand Gamanagatti, Associate Professor, Department of Radiology, JPNA Trauma Centre, All India Institute of Medical Sciences, Ansari Nagar, New Delhi 110029, India. shiv223@rediffmail.com
Telephone: +91-11-26594567 Fax: +91-11-26588641
Received: April 9, 2011 Revised: July 28, 2011
Accepted: August 4, 2011
Published online: September 28, 2011

Key words: Shoulder joint; Instability; Magnetic resonance imaging; Magnetic resonance arthrogram

Peer reviewers: Sudsriluk Sampatchalit, MD, Lieutenant Colonel, Radiology, Phramongutglao Royal Thai Army Hospital, 315 Ratchawithi Road, Ratchathewi, Bangkok 10400, Thailand; Wenbao Wang, MD, Orthopaedic Department, Columbia University Medical Center, 106 Fort Washington Avenue, Apt 3H, New York, NY 10032, United States

Jana M, Gamanagatti S. Magnetic resonance imaging in glenohumeral instability. *World J Radiol* 2011; 3(9): 224-232 Available from: URL: http://www.wjgnet.com/1949-8470/full/v3/i9/224.htm DOI: http://dx.doi.org/10.4329/wjr.v3.i9.224

Abstract

The glenohumeral joint is the most commonly dislocated joint of the body and anterior instability is the most common type of shoulder instability. Magnetic resonance (MR) imaging, and more recently, MR arthrography, have become the essential investigation modalities of glenohumeral instability, especially for pre-procedure evaluation before arthroscopic surgery. Injuries associated with glenohumeral instability are variable, and can involve the bones, the labor-ligamentous components, or the rotator cuff. Anterior instability is associated with injuries of the anterior labrum and the anterior band of the inferior glenohumeral ligament, in the form of Bankart lesion and its variants; whereas posterior instability is associated with reverse Bankart and reverse Hill-Sachs lesion. Multidirectional instability often has no labral pathology on imaging but shows specific osseous changes such as increased chondrolabral retroversion. This article reviews the relevant anatomy in brief, the MR imaging technique and the arthrographic technique, and describes the MR findings in each type of instability as well as common imaging pitfalls.

INTRODUCTION

Shoulder joint is the most mobile and most commonly dislocated joint of the body[1]. Injuries to this joint leading to dislocation, subluxation and fracture are common, especially in young active individuals. Glenohumeral instability can be classified differently (Table 1) based on the etiopathogenesis (traumatic or atraumatic), direction of dislocation (anterior or posterior) or chronicity (acute or chronic). Traumatic anterior instability (often represented by the term TUBS; Traumatic, Unidirectional, Bankart, Surgical) is the most common clinical entity compared to atraumatic multidirectional instability[1]. Anterior dislocation comprises the majority (95%) of all cases; whereas posterior dislocation is less common[1].

In this article, we will review the anatomy, the magnetic resonance imaging (MRI) techniques and recent advancements in imaging of glenohumeral instability, and commonly encountered abnormalities in glenohumeral instability.

ANATOMY

The shoulder girdle is comprised of three joints, the

Table 1 Classification of glenohumeral instability

Classification	Types of instability
Anatomic	Anterior
	Posterior
	Multidirectional
Etiologic	Traumatic (TUBS)
	Atraumatic (AMBRI)
Clinical course	Acute
	Recurrent
Degree of instability	Subluxation
	Dislocation

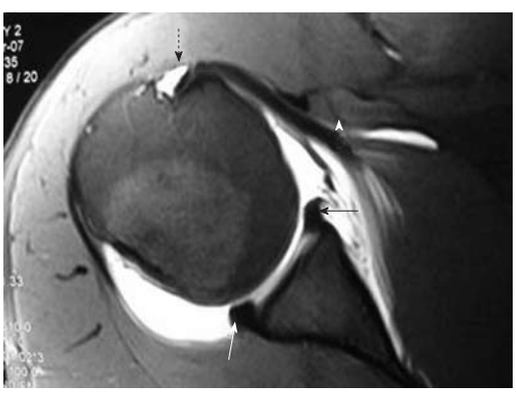

Figure 1 Normal T1-weighted TSE fat-saturated axial magnetic resonance arthrogram image. The anterior and posterior labrum appears as triangular hypointense structures (straight arrows). Normal middle glenohumeral ligament has been shown with an arrowhead. Note the long head of biceps tendon in the bicipital groove and extension of joint fluid around the tendon (dashed arrow).

glenohumeral joint, the acromioclavicular joint and the sternoclavicular joint. The glenohumeral joint, a ball- and socket type of joint, is the main component of the shoulder girdle mechanism[1]. The glenoid labrum is a fibrocartilage located at the glenoid rim which increases the depth by 2-4 mm (50%)[2] and increases the articular surface of the socket by 1 cm. Normal glenoid labrum appears as a triangular structure at the glenoid margin, having hypointense signal intensity on all sequences (Figure 1)[1]. Principal stabilizing mechanisms of the shoulder joint are the rotator cuff tendons (dynamic stabilizers) and the glenoid labrum and the ligaments (static stabilizers)[2]. The rotator cuff tendons are comprised of four tendons arranged around the shoulder girdle: the subscapularis, supraspinatus, infraspinatus, and teres minor. Normal tendons appear hypointense on T1-weighted (T1W) as well as T2-weighted (T2W) images[1,2].

Glenohumeral ligaments (superior, middle and inferior) are thickenings of the capsule of the glenohumeral joint. Normal glenohumeral ligaments appear as hypointense linear bands, best documented after joint distension on magnetic resonance (MR) arthrography (Figures 2-4). The inferior glenohumeral ligament (IGHL) is made up of two components, the anterior and the posterior bands[1,2]. The anterior band of the IGHL is of prime importance in the stability of the shoulder joint. The anterior inferior labrum and the anterior band of

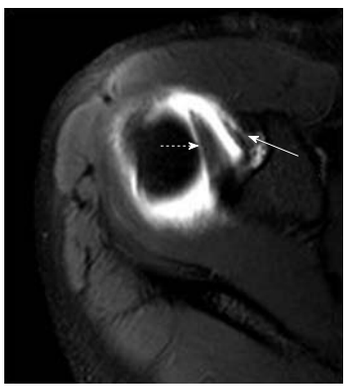

Figure 2 Axial T1-weighted fat-saturated magnetic resonance arthrogram image shows normal superior glenohumeral ligament (straight arrow) running parallel to the coracoid concavity and the long head of biceps tendon (dashed arrow).

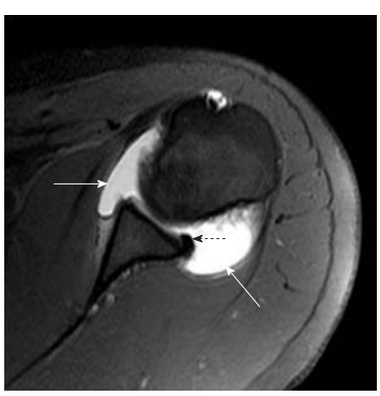

Figure 3 Axial T1-weighted fat-saturated magnetic resonance arthrogram image shows normal anterior and posterior bands of inferior glenohumeral ligament (straight arrows). Posterior labrum is seen as normal hypointense structure (dashed arrow), anterior labrum is congenitally absent in this patient.

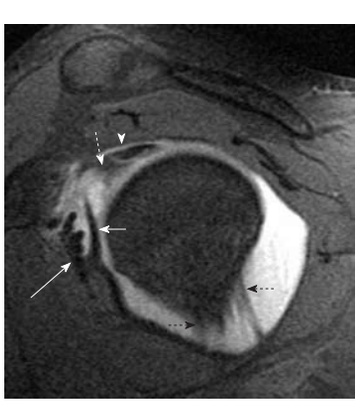

Figure 4 Oblique sagittal T1-weighted fat-saturated magnetic resonance arthrogram image shows normal superior glenohumeral ligament (white dashed arrow), inferior to the intra-articular long head of biceps tendon (arrowhead). The middle glenohumeral ligament is seen as a long hypointense band (short straight arrow) medial to the subscapularis tendon (long straight arrow). Anterior and posterior bands of inferior glenohumeral ligament are shown with black dashed arrows.

the IGHL are better visualized on oblique axial scan with the shoulder in abduction and external rotation (ABER)[3,4]. Inferior labral-ligamentous abnormalities

Table 2 Arthrographic techniques and their drawbacks

Arthrographic technique	Procedure	Advantages	Drawbacks
Indirect	Intravenous injection of gadolinium and imaging 10 min after active exercise of the joint	Simple Does not involve intra-articular injection	Joint cavity distension not achieved; ligamentous pathologies not well detected
Direct arthrography: anterior approach	Dilute gadolinium injected in the joint cavity through an anterior approach (US- or fluoroscopy-guided). Injection made through a point at the junction of the upper two-thirds and lower–third of anterior joint space	Adequate joint distension helps detection of labral and ligamentous pathologies better	Needs expertise May cause injury to the anterior stabilizing structures Carries the risk of intra-articular infection (though rare)
Direct arthrography: posterior approach	Dilute gadolinium injected in the joint cavity through a posterior approach (US- or fluoroscopy-guided)	Adequate joint distension helps detection of labral and ligamentous pathologies better May be helpful in anterior instability, to avoid injury to anterior structures	Needs expertise May cause injury to posterior structures Carries the risk of intra-articular infection (though rare)
Direct arthrography: anterosuperior approach	Dilute gadolinium injected in the joint cavity through an anterosuperior approach in the RCI (US- or fluoroscopy-guided)	Adequate joint distension helps detection of labral and ligamentous pathologies better	Needs expertise May cause injury to the rotator interval capsule

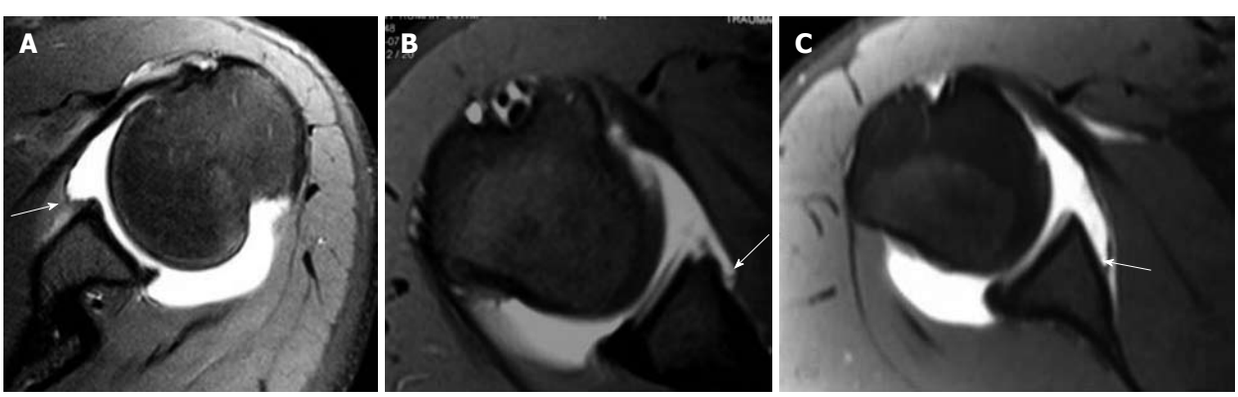

Figure 5 Magnetic resonance arthrographic axial T1-weighted fat-saturated images showing different types of attachment of anterior joint capsule. A: Type Ⅰ; B: Type Ⅱ; C: Type Ⅲ (arrows).

have been reported to be most closely correlated with anterior glenohumeral instability[5].

The attachment of the anterior joint capsule and middle glenohumeral ligament (MGHL) shows significant variability. Three types of attachment have been described: type I refers to an attachment of the anterior joint capsule at the anterior labral tip or at the base of the labrum; in type Ⅱ attachment, the capsule attaches to the glenoid close to the labral base; whereas type Ⅲ refers to an attachment more medially along the scapular neck (Figure 5)[6].

Rotator cuff interval (RCI) is defined as the discontinuity of the rotator cuff that occurs between the superior border of the subscapularis and the anterior border of the supraspinatus tendon (Figure 6). Structural insufficiency of its components and the overlying capsule caused by trauma can result in instability[7].

The long head of biceps tendon, after its origin from the supraglenoid tubercle, traverses a long intra-articular course through the superior part of the joint and the RCI before coursing through the bicipital groove. In cranial axial sections, it is seen as a linear hypointense structure coursing parallel to the superior glenohumeral ligament (SGHL) (Figure 2).

MRI TECHNIQUE IN SHOULDER INSTABILITY

Routine imaging of the shoulder is done in three planes. The acquisition of images in the oblique coronal plane, which is the single most important imaging plane in the shoulder joint, is done parallel to the supraspinatus tendon. Oblique sagittal images are acquired at a plane perpendicular to the plane of the glenoid face, and best planned on an axial image[1].

Articular cartilage and labrum are best evaluated on a proton density (PD) or gradient echo image on axial and oblique coronal planes. The rotator cuff tendons should be evaluated on oblique coronal and oblique sagittal planes. For evaluation of the signal intensity of the rotator cuff tendons, T2W fat-saturated images are ideal[1,2]. On oblique sagittal images, the entire rotator cuff tendons, muscles and RCI can be assessed. In the setting of trauma, T1W images are less helpful, and can be acquired in oblique coronal plane only[1].

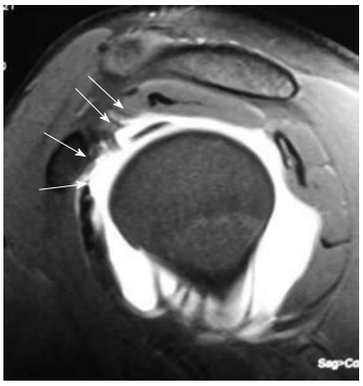

Figure 6 Oblique sagittal T1-weighted fat-saturated magnetic resonance arthrogram image shows normal rotator cuff interval (arrows).

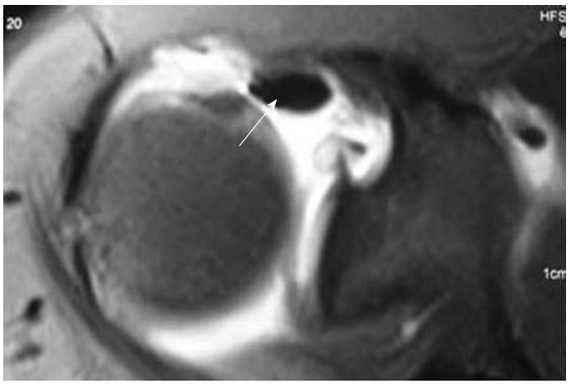

Figure 7 Axial T1-weighted fat-saturated magnetic resonance arthrogram image shows artifact due to inadvertent injection of air into the joint cavity. The air appears as hypointense structure lying in nondependent areas (arrow), which helps differentiate it from loose bodies.

MR ARTHROGRAPHY

MR arthrography has proven its utility in the evaluation of glenohumeral instability and cartilage abnormalities. MR arthrography can either be direct or indirect (Table 2). Direct MR arthrography procedure can be divided into two parts: injection of the dilute gadolinium contrast agent into the joint and imaging in a MR scanner. Usually fat-saturated T1W images are obtained in all three planes. The labrum and glenohumeral ligaments are well visualized after distension of the joint cavity by the intra-articular injection[8]. The only drawback of this imaging protocol is that it can miss the presence of any intra-substance rotator cuff tear. To avoid this difficulty, additional T2W MRI with fat suppression can be done in the oblique coronal plane. Imaging with the shoulder in ABER position increases the sensitivity and specificity of detection of anteroinferior labral and glenohumeral ligament attachment abnormalities[3].

The injecting approach in MR arthrography has undergone several alterations since its introduction. Injection can be performed either through anterior, anterosuperior or posterior approach. Anterior approach is the most commonly adopted one. In 1975, Schneider *et al*[9] described a simplified injection technique, which uses a straight anteroposterior approach with a 3.5 inch (8.8 cm), 22 gauge needle directed vertically at the junction of the middle and lower thirds of the glenohumeral joint under fluoroscopic guidance. After confirmation of needle placement using 1-2 mL iodinated contrast agent, 10-12 mL of a dilute gadolinium solution (1:200 dilution) is injected into the joint cavity. MR imaging is usually performed within 90 min to avoid absorption of the intra-articular contrast.

A posterior approach can also be adopted, especially when there is anterior instability as needle placement through an anterior route may distort the images of healthy anatomic structures[10]. The patient lies prone with ipsilateral shoulder raised off the table with a pad. A 21 gauge spinal needle is advanced vertically through the inferomedial aspect of the humeral head under fluoroscopic guidance.

For a long time, a modified Schneider technique (anterosuperior approach through rotator interval) has been in use, where the patient is kept supine with arm externally rotated and a 1.5 inch (3.8 cm), 20-22 gauge needle is inserted through an area medial to the superior third of the humeral head. The needle tip is advanced in an anteroposterior direction to the humeral head to avoid contact with the glenoid labrum. The utility of this procedure was established by Dépelteau *et al*[11].

In indirect MR arthrography, gadolinium is injected intravenously and imaging is done after it diffuses into the joint cavity through a highly vascular synovial lining (which takes a few minutes). However, it lacks the effect of joint distension (compared to direct MR arthrogram).

While performing MR arthrography, adequate precautions should be taken to avoid introduction of air in the joint cavity, which can mimic detached and torn labrum on imaging (Figure 7). The gadolinium concentration should also be properly checked, as injection of undiluted gadolinium may lead to diffuse low signal intensity in the joint cavity.

MRI FINDINGS IN SHOULDER INSTABILITY

MR imaging in anterior instability can reveal a large number of abnormalities affecting the bone and labroligamentous tissue.

Hill-Sachs lesion

Hill-Sachs lesion (Figure 8) is the most common injury associated with anterior glenohumeral instability. It consists of bony injury of the posterosuperior humeral head manifesting as cortical bony loss, impaction fracture or associated bone marrow edema in acute cases.

Classic bankart lesion

Bankart lesion (Figure 9) is the commonest labral injury, manifesting as tear of the anterior inferior labrum with associated periosteal tear[12-14]. It can be purely cartilaginous or may involve the bony glenoid rim (bony Bankart

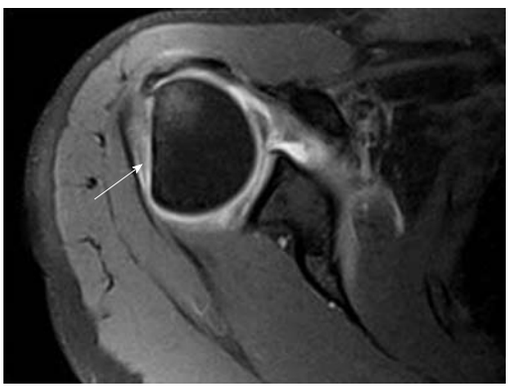

Figure 8 Axial T1-weighted TSE fat-suppressed magnetic resonance arthrogram image shows bony defect involving posterosuperior humeral head (Hill-Sachs lesion) (arrow).

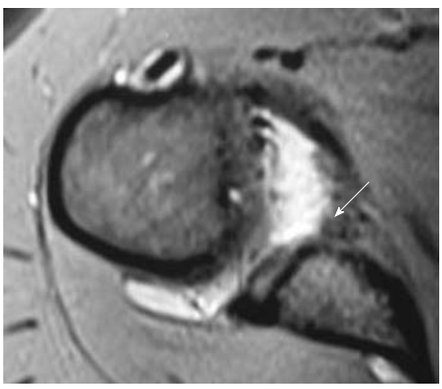

Figure 10 Axial T1-weighted TSE fat-suppressed magnetic resonance arthrogram image shows anteroinferior labral tear with bony glenoid injury shown with an arrow (Bony Bankart lesion).

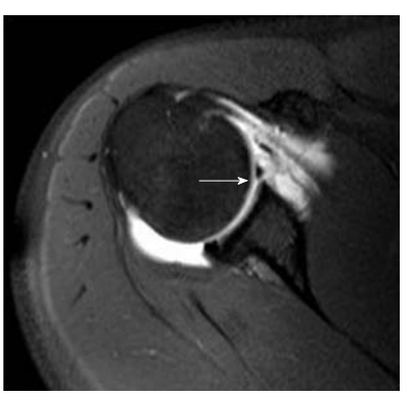

Figure 9 Axial T1-weighted TSE fat-suppressed magnetic resonance arthrogram image shows detached anteroinferior labrum from the glenoid margin; classic soft tissue Bankart lesion. Contrast within the joint is seen to traverse the gap between the detached labrum and the glenoid margin (arrow).

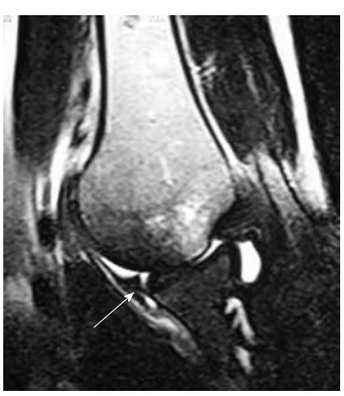

Figure 11 Perthes lesion. Oblique axial T2-weighted TSE image of the shoulder joint with the arm in abduction and external rotation location shows tear of the anteroinferior labrum (arrow) with intact periosteum, suggesting Perthes lesion.

lesion, Figure 10). Bankart lesion is usually accompanied by Hill-Sachs lesion. Several other variants of Bankart lesion have been described, including the Perthes lesion, anterior labroligamentous periosteal sleeve avulsion (ALPSA) lesion, glenolabral articular disruption (GLAD) lesion.

On conventional MR imaging in Bankart lesion, the anteroinferior labrum is seen to be attenuated or absent. The signal intensity on T2* gradient-echo or PD FS FSE MR images may be increased secondary to degeneration of the labrum. On T1 turbo spin echo fat stauration (TSE FS) post-arthrographic MR images, contrast is seen between the labrum and the glenoid margin.

Perthes lesion

Perthes lesion (Figure 11), described by Perthes in 1905, is defined as a tear of the glenoid labrum with intact scapular periosteum[15]. The torn anterior labrum is often undisplaced and visualized in its normal location on conventional MR imaging. MR arthrography, especially when imaging is performed with the arm in ABER position, improves the detection rate of Perthes lesion, as it puts the anterior band of the IGHL and anteroinferior capsule under stress. This is a difficult lesion to detect, both on conventional MRI and even on arthroscopy[12].

ALPSA lesion

ALPSA lesion (described by Neviaser[16]) is defined as an avulsion and medial rolling of the inferior labroligamentous complex along the scapular neck secondary to a chronic injury (Figure 12). The main differentiating point of ALPSA from a Perthes lesion is the displacement of the torn labroligamentous tissue, which is undisplaced or shows minimal displacement in Perthes lesion. An ALPSA lesion differs from a Bankart lesion in that an ALPSA lesion has an intact anterior scapular periosteum (it is ruptured in Bankart lesion) that allows the labroligamentous structures to displace medially and rotate inferiorly on the scapular neck.

GLAD lesion

This lesion (also described by Neviaser[17]) consists of a superficial anterior inferior labral tear associated with an anterior inferior articular cartilage injury (Figure 13). The use of intra-articular contrast in MR arthrogram helps to visualize the small tears at the level of the anterior inferior glenoid rim. When a GLAD lesion is seen on MRI, one should look for loose bodies, which can occur from

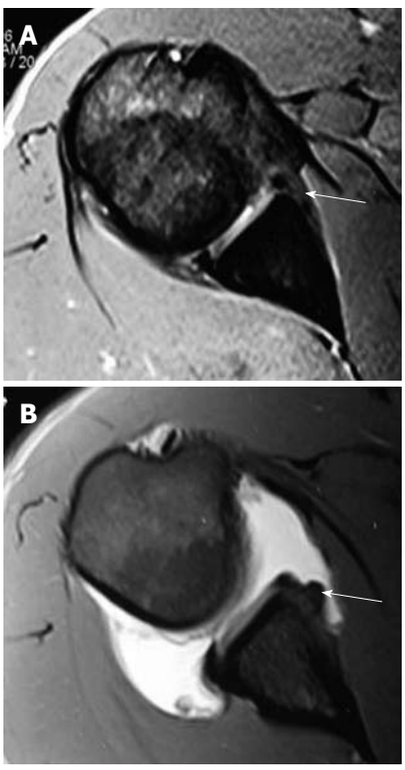

Figure 12 Anterior labroligamentous periosteal sleeve avulsion lesion in a patient with recurrent anterior shoulder dislocation. A: Axial T2-weighted gradient-echo image of the right shoulder reveals irregular contour of the anteroinferior labrum and hypointense soft tissue lying along the scapular neck (arrow); B: On magnetic resonance arthrographic axial T1-weighted fat-saturated image the avulsed labroligamentous tissue is seen displaced medially along the scapular neck (arrow).

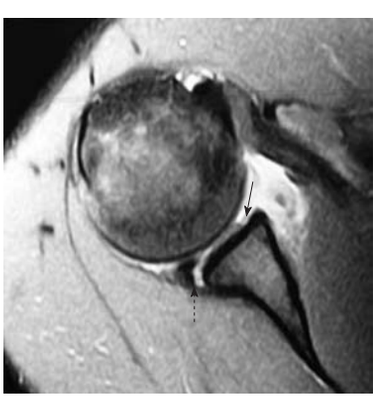

Figure 13 Glenolabral articular disruption lesion and posterior labral tear in a patient with multidirectional instability. Axial proton density fat-suppressed image reveals absence of the anteroinferior labrum with tear of the adjacent articular cartilage (straight arrow). Also associated is a tear involving the posterior labrum, seen as interposition of fluid between the posterior labrum and the posterior glenoid margin (dashed arrow).

a detached articular cartilage fragment[18].

Superior labrum anterior and posterior type 5 lesion

Superior labrum anterior and posterior (SLAP) lesion, described by Snyder *et al*[19], is an injury involving the superior aspect of the glenoid labrum that includes the biceps tendon anchor. SLAP tears were initially classified by Snyder *et al*[19] into 4 distinct but related lesions; Maffet *et al*[20] added three more types, and currently 10 types or patterns have been recognized. Though SLAP lesions often present with nonspecific symptoms such as pain, locking and snapping, type 5 SLAP lesion (type 2 or 3 SLAP lesion with superior extension of a Bankart lesion) is often associated with anterior shoulder dislocation. Sagittal MRI or MR arthrogram can demonstrate the complete extent of labral tear.

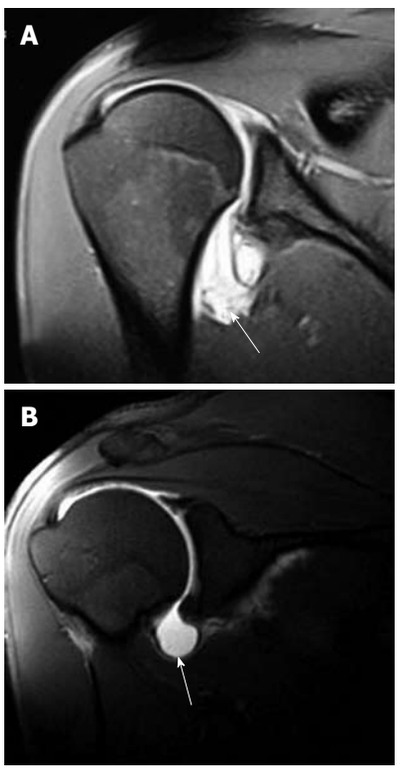

Figure 14 Humeral avulsion of anterior glenohumeral ligament in chronic anterior instability. Coronal T1-weighted TSE fat-suppressed magnetic resonance arthrogram image reveals the 'J' shape (arrow) of the axillary pouch (A), compared to the 'U' shape (arrow) in a normal individual (B).

Humeral avulsion of anterior glenohumeral ligament lesion

Humeral avulsion of anterior glenohumeral ligament (HAGL) lesion (Figure 14) is a less commonly encountered abnormality (9.3%) in anteroinferior instability[21]. It may coexist with an anterior labral tear in patients with anterior instability. In patients with documented anterior instability without a demonstrable "primary" Bankart lesion, a HAGL lesion should be ruled out[14]. For detection of HAGL, the glenohumeral joint cavity should be well distended, either by contrast agent (direct MR arthrogram) or joint effusion. On coronal MR image, normal distended axillary pouch is seen as a U-shaped structure, which changes into a J-shape in a HAGL lesion as the IGHL drops inferiorly (J sign)[22].

Bony humeral avulsion of glenohumeral ligaments lesion

Bony humeral avulsion of glenohumeral ligaments (BHA-

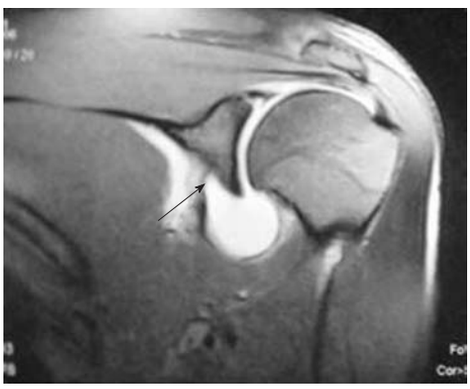

Figure 15 Glenolabral articular disruption lesion. Coronal T1-weighted TSE fat-suppressed magnetic resonance arthrogram image reveals avulsion of the glenoid attachment of the anterior band of the inferior glenohumeral ligament (arrow).

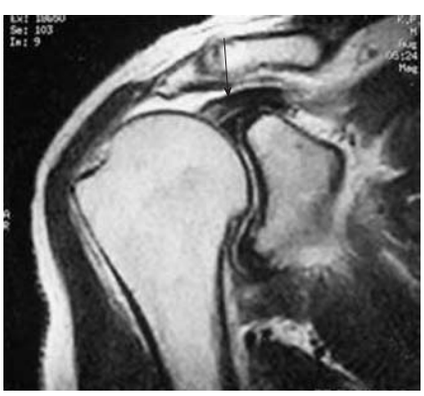

Figure 16 Coronal TSE T2-weighted image of the right shoulder in a patient with acute dislocation reveals full thickness tear of the supraspinatus tendon with proximal retraction of the muscle (arrow).

GL) lesion is less common than HAGL. In BHAGL, there is a small avulsed osseous fragment attached to the torn end of the humeral attachment of the IGHL[23].

GAGL lesion

This uncommon lesion implies an avulsion of the IGHL from the inferior pole of glenoid without associated disruption of the inferior labrum (Figure 15)[2].

Rotator cuff tears

These tears (Figure 16), associated with anterior and inferior glenohumeral dislocation, are commoner in the elderly rather than the younger age group (30% incidence in patients less than 40 years of age and 80% incidence above 60 years of age).

RCI tear

A tear of the RCI typically does not appear as complete disruption of the fibres of its components. Instead it is seen on imaging as thinning, irregularity or focal discontinuity of the rotator interval capsule. Arthroscopy is considered the gold standard in diagnosing RCI lesions. MR arthrography, particularly the T2W sagittal or axial images, may be useful in diagnosing RCI pathologies.

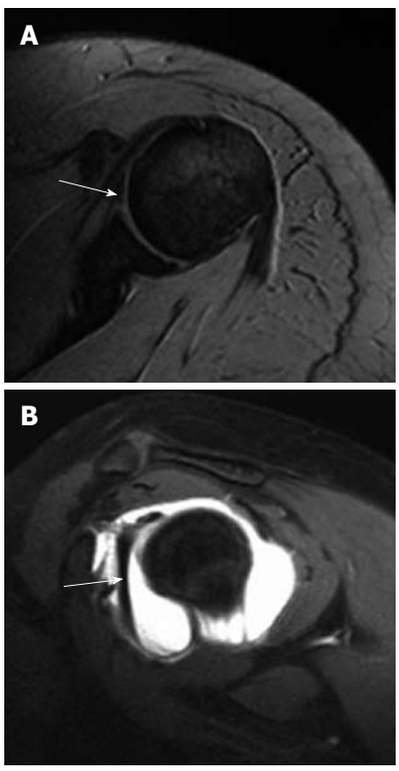

Figure 17 Buford complex. A: Axial T2-weighted gradient-echo image reveals absent anterior labrum and a thick hypointense structure lying anteriorly (arrow) which can be mistaken for a torn labrum; B: Oblique sagittal T1-weighted TSE fat-saturated magnetic resonance arthrogram image reveals a thick cord-like middle glenohumeral ligament (arrow) having a higher glenoid attachment, close to 12 o'clock location.

ANATOMIC VARIATIONS MIMICKING LABRAL TEARS

Sublabral foramen is a normal detachment of the anterosuperior labrum (usually at 2 o'clock location) from the glenoid rim that needs to be differentiated from a Bankart lesion[24]. Bankart lesion usually involves the anteroinferior labrum (isolated anterosuperior labral involvement is rare and seen in throwing athletes presenting with pain on overhead abduction). The margins of a labral tear are usually irregular as compared to the sublabral foramen.

Buford complex (Figure 17) is defined as congenital absence of the anterosuperior labrum and thickened cord-like MGHL. The thickened MGHL, when visualized on axial MR images, can mimic detached labrum of a Bankart lesion. However, on oblique sagittal arthrographic images, the superior insertion of a cord-like MGHL is usually visible and misdiagnosis can be avoided[24].

IMAGING FINDINGS IN POSTERIOR DISLOCATION

Reverse hill-sachs lesion

This lesion (Figure 18) consists of an anteromedial superior humeral head impaction fracture which is often associated with a reverse Bankart lesion (posterior glenoid labrum disruption)[25].

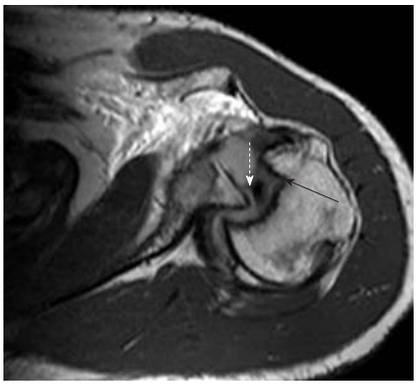

Figure 18 Reverse Hill-Sachs and reverse Bankart lesion in a case of posterior instability. T1-weighted TSE axial magnetic resonance image reveals hemarthrosis, posterior glenohumeral dislocation and reverse Hill-Sachs lesion (straight arrow). There is associated posterior labral tear (reverse Bankart lesion), shown with a dashed arrow.

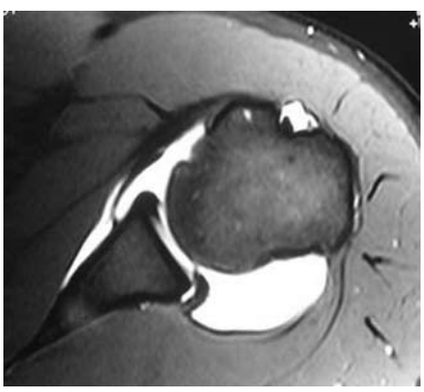

Figure 19 Posterior labral tear. Axial T1-weighted TSE fat-suppressed magnetic resonance arthrogram image reveals the undisplaced posterior labral tear (arrow). The anterior joint capsule attachment is placed medially along scapular neck (normal variation).

Reverse hagl lesion

In posterior instability, there is sometimes a complete avulsion of the posterior attachment of the shoulder capsule from the posterior humeral neck, associated with tear of the posterior band of the IGHL[4].

Posterior glad lesion

This lesion is a newly described entity in posterior glenohumeral instability, which can be seen as focal posterior articular cartilage defect (between 7 and 9 o'clock location)[26].

Bennett lesion

This is an extra-articular crescentic posterior ossification associated with posterior labral injury and capsular avulsion, sometimes secondary to the posterior subluxation. The ossification is best visualized on CT, and often missed by arthroscopy as it is extra-articular.

Posterior superior labral tear

This occurs (Figure 19) as a part of posterior SLAP 2 or posterosuperior to a posterior labral tear in association with a paralabral cyst and may be seen in patients with posterior instability. Posterior superior labral tear may be associated with repetitive microtrauma, as in throwers, and can even be seen in anterior instability[27]. The cysts are almost always associated with labral tears, but the communication with the joint space is often not visualized on MRI.

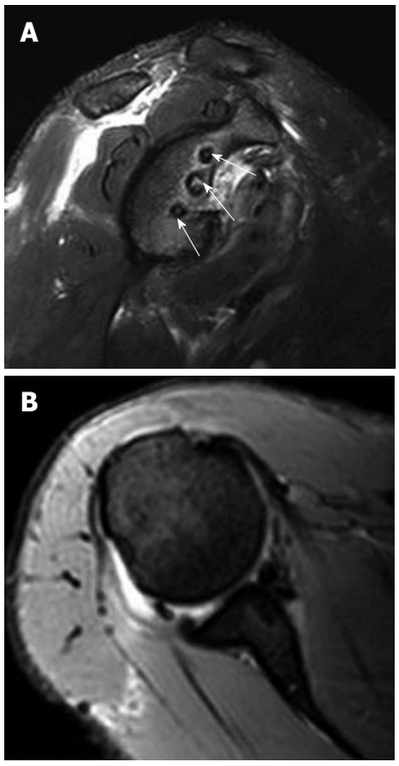

Figure 20 Normal post-operative appearance after arthroscopic suture-anchor repair of Bankart lesion. Oblique sagittal (A) and axial (B) T2-weighted TSE fat-suppressed image reveals the three suture-anchors in place (arrows). No fluid is seen between the labral margin and the opposed labrum and joint capsule.

POST-OPERATIVE IMAGING

Anatomic repair of the labrum and capsule using metallic suture anchors is being increasingly employed in glenohumeral instability using an arthroscopic approach[28]. On post-operative MR imaging, susceptibility artifacts (Figure 20) from the metallic implants may degrade the image quality. A few important points should be kept in mind to overcome this problem: gradient echo sequences should be avoided and replaced by spin echo sequences when possible; fast spin echoes are preferable over standard spin echo sequences; and inversion recovery sequences should be preferred over chemical fat suppression. After an anatomic apposition of the labrum to the articular margin in suture-anchor repair, no hyperintensity should be visible between the two. MR arthrography is more useful in post-operative shoulders as a problem solving tool in suspected recurrent labral tear. Contrast-enhanced T1W sequences should always be acquired in addition if there is a suspicion of septic arthritis[29].

Non-anatomic repairs (Putti-Platt repair, Bristow-

Helfet procedure) are usually not preferred for primary instability surgery. Following capsular shift or shrinkage procedures, thickening of the joint capsule can be visualized on imaging.

Complications during arthroscopic repair include inadvertent injury to the axillary nerve (lying in close relation to the inferior joint capsule) and subscapularis muscle injury, hematoma, infection, septic arthritis, heterotopic ossification.

RECENT ADVANCES IN SHOULDER MRI

Virtual MR arthroscopy of the shoulder joint has been described in a few reports using 3D gradient echo sequences after intra-articular injection of dilute gadolinium[30]. The technique can act as a useful adjunct tool to MR arthrography in the assessment of labral tears, by providing helpful visual information similar to arthroscopy.

CONCLUSION

To conclude, MRI and MR arthrography are routinely used investigations in glenohumeral instability and have very high sensitivity in detecting labroligamentous injuries. An MR arthrogram plays a crucial role in the imaging of post-operative shoulder. While diagnosing various labral lesions, anatomic variations should be kept in mind.

REFERENCES

1 **Tirman PFJ**. Glenohumeral instability. In: Steinbach LS, Tirman PFJ, Peterfy CG, Feller JF, editors. Shoulder magnetic resonance imaging. Philadelphia: Lippincott-Raven, 1998: 135-167
2 **Stoller DW**, Wolfe EM, Li AE, Nottage WM, Tirman PFJ. The shoulder. In: Stoller DW, editor. Magnetic resonance imaging in orthopedics and sports medicine. 3rd ed. Philadelphia, PA: Lippincott Williams and Wilkins, 2007: 1131-1462
3 **Cvitanic O**, Tirman PF, Feller JF, Bost FW, Minter J, Carroll KW. Using abduction and external rotation of the shoulder to increase the sensitivity of MR arthrography in revealing tears of the anterior glenoid labrum. *AJR Am J Roentgenol* 1997; **169**: 837-844
4 **Chung CB**, Sorenson S, Dwek JR, Resnick D. Humeral avulsion of the posterior band of the inferior glenohumeral ligament: MR arthrography and clinical correlation in 17 patients. *AJR Am J Roentgenol* 2004; **183**: 355-359
5 **Palmer WE**, Caslowitz PL. Anterior shoulder instability: diagnostic criteria determined from prospective analysis of 121 MR arthrograms. *Radiology* 1995; **197**: 819-825
6 **Massengill AD**, Seeger LL, Yao L, Gentili A, Shnier RC, Shapiro MS, Gold RH. Labrocapsular ligamentous complex of the shoulder: normal anatomy, anatomic variation, and pitfalls of MR imaging and MR arthrography. *Radiographics* 1994; **14**: 1211-1223
7 **Bigoni BJ**, Chung CB. MR imaging of the rotator cuff interval. *Magn Reson Imaging Clin N Am* 2004; **12**: 61-73, vi
8 **Palmer WE**, Brown JH, Rosenthal DI. Labral-ligamentous complex of the shoulder: evaluation with MR arthrography. *Radiology* 1994; **190**: 645-651
9 **Schneider R**, Ghelman B, Kaye JJ. A simplified injection technique for shoulder arthrography. *Radiology* 1975; **114**: 738-739
10 **Chung CB**, Dwek JR, Feng S, Resnick D. MR arthrography of the glenohumeral joint: a tailored approach. *AJR Am J Roentgenol* 2001; **177**: 217-219
11 **Dépelteau H**, Bureau NJ, Cardinal E, Aubin B, Brassard P. Arthrography of the shoulder: a simple fluoroscopically guided approach for targeting the rotator cuff interval. *AJR Am J Roentgenol* 2004; **182**: 329-332
12 **Waldt S**, Burkart A, Imhoff AB, Bruegel M, Rummeny EJ, Woertler K. Anterior shoulder instability: accuracy of MR arthrography in the classification of anteroinferior labroligamentous injuries. *Radiology* 2005; **237**: 578-583
13 **Rowan KR**, Keogh C, Andrews G, Cheong Y, Forster BB. Essentials of shoulder MR arthrography: a practical guide for the general radiologist. *Clin Radiol* 2004; **59**: 327-334
14 **Shankman S**, Bencardino J, Beltran J. Glenohumeral instability: evaluation using MR arthrography of the shoulder. *Skeletal Radiol* 1999; **28**: 365-382
15 **Wischer TK**, Bredella MA, Genant HK, Stoller DW, Bost FW, Tirman PF. Perthes lesion (a variant of the Bankart lesion): MR imaging and MR arthrographic findings with surgical correlation. *AJR Am J Roentgenol* 2002; **178**: 233-237
16 **Neviaser TJ**. The anterior labroligamentous periosteal sleeve avulsion lesion: a cause of anterior instability of the shoulder. *Arthroscopy* 1993; **9**: 17-21
17 **Neviaser TJ**. The GLAD lesion: another cause of anterior shoulder pain. *Arthroscopy* 1993; **9**: 22-23
18 **McCauley TR**. MR imaging of the glenoid labrum. *Magn Reson Imaging Clin N Am* 2004; **12**: 97-109, vi-vii
19 **Snyder SJ**, Karzel RP, Del Pizzo W, Ferkel RD, Friedman MJ. SLAP lesions of the shoulder. *Arthroscopy* 1990; **6**: 274-279
20 **Maffet MW**, Gartsman GM, Moseley B. Superior labrum-biceps tendon complex lesions of the shoulder. *Am J Sports Med* 1995; **23**: 93-98
21 **Wolf EM**, Cheng JC, Dickson K. Humeral avulsion of glenohumeral ligaments as a cause of anterior shoulder instability. *Arthroscopy* 1995; **11**: 600-607
22 **Carlson CL**. The "J" sign. *Radiology* 2004; **232**: 725-726
23 **Oberlander MA**, Morgan BE, Visotsky JL. The BHAGL lesion: a new variant of anterior shoulder instability. *Arthroscopy* 1996; **12**: 627-633
24 **McCarthy C**. Glenohumeral instability. *Imaging* 2003; **15**: 174-179
25 **Harish S**, Nagar A, Moro J, Pugh D, Rebello R, O'Neill J. Imaging findings in posterior instability of the shoulder. *Skeletal Radiol* 2008; **37**: 693-707
26 **Anderson M**, Barr M, Gaskin C, Alford B. Posterior GLAD lesions of the shoulder (scientific Presentation). Radiological Society of North America 2005
27 **Hottya GA**, Tirman PF, Bost FW, Montgomery WH, Wolf EM, Genant HK. Tear of the posterior shoulder stabilizers after posterior dislocation: MR imaging and MR arthrographic findings with arthroscopic correlation. *AJR Am J Roentgenol* 1998; **171**: 763-768
28 **Zlatkin MB**. MRI of the postoperative shoulder. *Skeletal Radiol* 2002; **31**: 63-80
29 **Mohana-Borges AV**, Chung CB, Resnick D. MR imaging and MR arthrography of the postoperative shoulder: spectrum of normal and abnormal findings. *Radiographics* 2004; **24**: 69-85
30 **Song HT**, Huh YM, Kim S, Kim SJ, Suh JS. The usefulness of virtual MR arthroscopy as an adjunct to conventional MR arthrography in detecting anterior labral lesions of the shoulder. *AJR Am J Roentgenol* 2009; **192**: W149-W155

S- Editor Cheng JX **L- Editor** Logan S **E- Editor** Zheng XM

World Journal of Radiology

Online Submissions: http://www.wjgnet.com/1949-8470office
wjr@wjgnet.com
doi:10.4329/wjr.v3.i9.233

World J Radiol 2011 September 28; 3(9): 233-240
ISSN 1949-8470 (online)

BRIEF ARTICLE

Assessment of contralateral mammary gland dose in the treatment of breast cancer using accelerated hypofractionated radiotherapy

Maria Tolia, Kalliopi Platoni, Andreas Foteineas, Maria-Aggeliki Kalogeridi, Anna Zygogianni, Nikolaos Tsoukalas, Mariangela Caimi, Niki Margari, Maria Dilvoi, Panagiotis Pantelakos, John Kouvaris, Vassilis Kouloulias

Maria Tolia, Kalliopi Platoni, Andreas Foteineas, Maria-Aggeliki Kalogeridi, Anna Zygogianni, Maria Dilvoi, Panagiotis Pantelakos, John Kouvaris, Vassilis Kouloulias, 1st and 2nd Department of Radiology, Radiation Oncology Unit, Medical School, Athens 12462, Greece
Nikolaos Tsoukalas, Oncology Clinic, 401 Military Hospital, Athens 11525, Greece
Mariangela Caimi, Department of Radiation Oncology, San Raffaele Hospital, Milan 20132, Italy
Niki Margari, Department of Cytology, Medical School, Athens 12462, Greece
Author contributions: Tolia M, Platoni K, Fotineas A, Kalogeridi MA, Zygogianni A, Dilvoi M and Kouloulias V performed the measurements, collected the data and wrote the Results and Discussion sections; Tolia M, Tsoukalas N, Caimi M, Margari N and Pantelakos P wrote the Introduction and Methods and Materials sections; Kouvaris J made the final edit.
Correspondence to: Dr. Maria Tolia, 2nd Department of Radiology, Radiation Oncology Unit, Medical School, Athens 12462, Greece. mariatolia@yahoo.gr
Telephone: +30-21-5831860 Fax: +30-21-5326418
Received: January 15, 2011 Revised: July 18, 2011
Accepted: July 25, 2011
Published online: September 28, 2011

Abstract

AIM: To measure the dose distribution, related to the treatment planning calculations, in the contralateral mammary gland of breast cancer patients treated with accelerated hypofractionated 3-dimensional conformal radiotherapy.

METHODS: Thirty-four prospectively selected female patients with right breast cancer (pN0, negative surgical margins) were treated with breast-conserving surgery. A total dose of 42.5 Gy (2.66 Gy/fraction) was prescribed; it was requested that planning target volumes be covered by the 95% isodose line. The contralateral mammary gland was defined on CT simulation. The dose received was evaluated by dose volume histograms.

RESULTS: The measured contralateral breast doses were: (1) Dose maximum: 290-448 cGy [Equivalent (Eq) 337-522 cGy]; (2) Mean dose: 45-70 cGy (Eq 524-815 cGy); and (3) Median dose: 29-47 cGy (337-547 cGy) for total primary breast dose of 42.5 Gy in 16 equal fractions. The spearman rho correlation showed statistical significance between the contralateral breast volume and maximum dose (P = 0.0292), as well as mean dose (P = 0.0025) and median dose (P = 0.046) to the breast.

CONCLUSION: Minimizing the dose to the contralateral breast has to be one of the priorities of the radiation oncologist when using short schedules because of the radiosensitivity of this organ at risk. Further study is necessary to assess the long-term clinical impact of this schedule.

Key words: Breast cancer; Hypofractionation; Contralateral breast; Dose calculation

Peer reviewer: Cem Onal, MD, Department of Radiation Oncology, Adana Research and Treatment Centre, Baskent University Medical Faculty, 01120 Yuregir, Adana, Turkey

Tolia M, Platoni K, Foteineas A, Kalogeridi MA, Zygogianni A, Tsoukalas N, Caimi M, Margari N, Dilvoi M, Pantelakos P, Kouvaris J, Kouloulias V. Assessment of contralateral mammary gland dose in the treatment of breast cancer using accelerated hypofractionated radiotherapy. *World J Radiol* 2011; 3(9): 233-240 Available from: URL: http://www.wjgnet.com/1949-8470/full/v3/i9/233.htm DOI: http://dx.doi.org/10.4329/wjr.v3.i9.233

INTRODUCTION

Breast cancer is the most common (excluding skin) malignant neoplasm among women. In the United States, it was calculated to have an approximate lifetime risk of 13.4%; 184 450 cases are invasive and 67 770 cases are *in situ* carcinomas per year[1].

The purpose of radiation treatment following lumpectomy is to improve local control in the treated breast with as little toxicity as possible. Since radiation therapy efficacy has improved, the issues related to post-therapy complications have become very important. Contralateral breast dose from primary breast irradiation has been implicated in the risk of second breast malignancies.

Daily treatment over several weeks can be very inconvenient to many patients. A high number of studies[2-13] have shown that the goal of post-lumpectomy radiotherapy is also achieved with shorter than the conventional fractionation schedules. Whole breast radiotherapy for invasive breast cancer demonstrates equivalent efficacy and morbidity for conventional and hypofractionated treatment, as shown in a Canadian trial involving 1234 women with node-negative breast cancer and clear margins of excision after breast conserving surgery and axillary dissection. Women were randomly assigned to receive whole breast irradiation of 42.5 Gy in 16 fractions over 22 d (short arm) or 50 Gy in 25 fractions over 35 d (long arm).

Hypofractionation can increase the late normal tissue damage. The principal long-term effects that impair cosmesis are fibrosis and atrophy of the breast which are a result of the specific response of fibrocytes to irradiation.

The aim of the present study was to evaluate the delivery of accelerated hypofractionated 3-D conformal radiotherapy (3D-CRT) in the contralateral mammary gland in breast cancer patients.

MATERIALS AND METHODS

Patient selection

Between October 2009 and September 2010, 34 women with a primary diagnosis of invasive carcinoma were enrolled in the treatment protocol. In the study were included patients > 50 years old, diagnosed with stage Ⅰ-Ⅱ, right-sided breast cancer. Large mammary glands with a distance from sternum to mid axillary line more than 25 cm were excluded from the study.

All patients underwent breast-conserving surgery (with axillary sampling or dissection). In particular, they had a lumpectomy before radiotherapy. They had no adjuvant chemotherapy. Exclusion criteria included previous treatment for a diagnosis of ductal carcinoma *in situ* or invasive breast carcinoma, omission of post-operative radiation, or surgical management with mastectomy.

Pathological results were abstracted from the original histopathology report. The specimens showed an invasive adenocarcinoma, non-high grade, negative margins (> 2 mm), no axillary lymph nodes involved.

Simulation

Each patient underwent a virtual CT-simulation, in supine position, using dedicated devices. The patient's arms were raised above the head using an arm support in carbon fiber (Sinmed©, Reeuwijk, The Netherlands).

Planning CT scans

For treatment planning, a CT scan covering a region from the 6th cervical vertebra to the middle part of the abdomen was obtained for each patient. The patients were scanned with 5 mm slice thickness in simulation CT scan and the CT datasets were transferred to the Prosoma® Treatment Planning System through the DICOM network.

Contouring organs at risk and planning target volume

All contouring of target volumes and normal structures [organs at risk (OARs)] were performed in the Prosoma Treatment Planning System. The following structures were delineated: clinical target volume (CTV), planning target volume (PTV), ipsilateral, contralateral lungs and contralateral breast. According to the ICRU[14,15], OAR is defined to be an uninvolved organ that, if given an excess radiation dose, might be damaged and would compromise the success of the course of radiation therapy.

The demonstrable tumor plus the microscopic disease constitute the CTV.

Margins are needed to surround the CTV to ensure that the CTV lies within the treatment field during the entire course of radiation therapy. These internal margins, in addition to the CTV, constitute the internal target volume (ITV).

In order to account for setup uncertainties, one adds a setup margin to the ITV to generate a PTV.

The CTV, PTV and OARs were outlined on all CT slices. The CTV was expanded to a PTV with 5 mm, with a constraint reverse expansion of 4 mm to the skin surface to avoid potential skin toxicity[16,17]. The PTV provided a margin around the CTV to compensate for the variability of treatment setup and motion of the breast or chest with breathing[17].

Dose prescription

The patients were treated with adjuvant whole breast radiotherapy and they received no boost and no supraclavicular irradiation. Radiation therapy to the involved breast was planned to be administered within 12 wk of the most recent surgery. A dose of 42.5 Gy was delivered in 16 daily fractions over 3.5 wk (2.66 Gy/fraction, based on the Canadian randomized trial)[2,3]. Breast radiation was delivered using tangential fields to the entire breast and underlying chest wall, as previously described. The prescription dose of 42.5 Gy was defined for the 95% isodoses of the PTV. In particular, 95% of the PTV should have been covered within 95%-110% of the prescribed dose (39.9-46.2 Gy). Partial wedging or dynamic (Multi Leaf Collimator-MLC) was employed to improve dose homogeneity (7%). To evaluate the dose constraints

for normal tissues we used the Toxicity criteria of the Radiation Oncology Group (RTOG) and the European Organization for Research and Treatment of Cancer (EORTC) NSABP B-39/RTOG 0413 protocol[18] corrected for hypofractionation, taking into account potential unfavorable anatomy[19]. The dose constraints for the OARs are described below: ipsilateral lung (without supraclavicular irradiation): V25 Gy < 5%, V17 Gy < 8%, V8 Gy < 10%, mean dose < 6.36 Gy; contralateral lung: V2.5 Gy < 15%; contralateral breast: dose max < 3% of the prescribed dose, mean dose as low as possible.

Conventional planning

For the conventional technique, we used a virtual simulation. The entire breast was treated, using a parallel pair of two opposed tangential fields. Weighted beams and wedges were used as necessary. The fields were placed isocentrically, with matching posterior field borders. Dose calculation was performed and normalized to isocenter. The prescribed dose was 42.5 Gy delivered in 16 daily fractions, in whole-breast, given in 2.66 Gy fractions with accelerated hypofractionated 3D-CRT[20].

The treatment planning was performed in the Eclipse™ (Varian Medical Systems, United States) TPS. This treatment planning system includes the Pencil Beam algorithm for dose calculation. The beam arrangement consisted of 2 tangential beams, where the beam angles, apertures, weights and dynamic wedges were optimized by standard, forward planning. The photon beam energy was 6 MV, using the linear accelerator VARIAN 600C. To account for the tumor movement during treatment, 2 cm was extended beyond the skin surface in the anterior direction using the skin flash tool in the treatment planning system.

For the treatment technique, histograms of the contralateral breast were generated; a number of parameters, including mean, median and maximum dose to the breast, were evaluated.

Clinical examination

During the radiation treatment the patients were monitored every week. Post treatment management included adjuvant endocrine therapy according to the National Comprehensive Cancer Network Guidelines. After the completion of the treatment, the patients were evaluated by a radiation oncologist every 3 mo. Acute skin and breast tissue reactions were also recorded. Toxicity was defined according to the RTOG/EORTC acute and late radiation morbidity scoring system[21].

Statistical analysis

Correlation of numerical variables was investigated by Pearson correlation coefficient. The whole analysis was performed by using the SPSS version 10 (Chicago, IL).

RESULTS

Thirty-four eligible women treated with adjuvant radiation following breast-conserving surgery were analyzed. The median age of the patients at the time of radiation was 65 years (range, 51-79 years). All patients underwent breast-conserving surgery with accompanying axillary sampling or dissection. All completed adjuvant whole breast radiotherapy with hypofractionated schedule (42.5 Gy in 16 fractions). Clinical and pathological characteristics were similar among the patients.

Table 1 Contralateral breast treatment characteristics

Treatment characteristics	Range
Dose max	290-448 cGy
Mean dose	45-70 cGy
Median dose	29-47 cGy
Monitor units	199-217
Breast volume	749-1474 cm^3

Table 2 Statistical analysis

Correlation	Spearman rho	*P* value
Breast volume *vs* max dose to the breast	0.0090	0.0292
Breast volume *vs* mean dose to the breast	0.0153	0.0025
Breast volume *vs* median dose to the breast	0.0028	0.046
Breast volume *vs* gantry angle	0.0042	0.2195

The doses to the opposite breast were generated from the dose volume histograms (DVHs) (Table 1). The doses represent the combined contribution from both the medial and lateral tangential beams. An isocentric technique was used for treatment. Scatter dose from the medial tangential field to the contralateral breast originates in the accelerator head and its accessories. The use of a medial wedge increased the contralateral breast dose due to an increase in scattered photons and in monitor units. The wedge angle used in our study ranged between 15° and 30°. For total primary dose of 4256 cGy, the measured dose maximum at the contralateral gland varies from 290-448 cGy. The mean dose varies from 45 to 70 cGy. The median dose was between 29-47 cGy. The average volume of the breast for the patients in question was 856 ± 327 cm^3. The monitor units obtained from the pencil beam calculations and used for the treatment were in the range from 199 to 217. A representative dose distribution for the breast with the contralateral breast contouring is shown in Figure 1 with regard to axial and coronal planes. A representative cumulative dose volume histogram is shown in Figure 2. The spearman rho correlation showed statistical significance between the contralateral breast volume and maximum dose ($P = 0.0292$), as well as mean dose ($P = 0.0025$) and median dose ($P = 0.046$) to the breast (Table 2). Received doses in detail as extracted from DVHs are shown in Table 3.

DISCUSSION

The choice of treatment for breast cancer is usually determined by tumor stage, patient age, co-morbidity, as well as by patient preferences. The long duration of treat-

Table 3 Calculated doses, breast volume and monitor units in details

No.	Age (yr)	Breast volume (cm^3)	Breast dose (cGy)			
			Max	Mean	Median	MU
1	79	1474	348	49	31	217
2	55	1090	380	45	41	209
3	63	803	367	54	47	203
4	61	749	290	45	35	199
5	71	789	448	63	46	203
6	56	857	345	56	36	204
7	67	942	401	47	32	210
8	72	801	412	52	39	200
9	61	998	434	51	40	202
10	56	796	399	52	45	210
11	58	893	387	45	33	199
12	72	956	402	70	33	204
13	71	1001	345	55	41	207
14	79	842	204	49	39	204
15	64	865	341	51	38	207
16	57	789	296	57	40	209
17	66	985	356	68	32	205
18	73	934	298	54	30	209
19	75	924	304	57	39	200
20	76	1023	326	61	45	210
21	59	1031	348	49	42	210
22	52	1320	401	51	40	211
23	57	980	295	59	32	205
24	58	1002	432	57	34	206
25	74	1007	422	49	37	209
26	70	983	427	61	40	200
27	60	879	346	58	40	204
28	74	765	307	49	38	214
29	68	795	401	60	39	208
30	72	1021	397	50	32	201
31	70	784	350	63	29	205
32	59	788	386	57	36	201
33	62	901	409	55	42	209
34	67	854	297	70	45	202

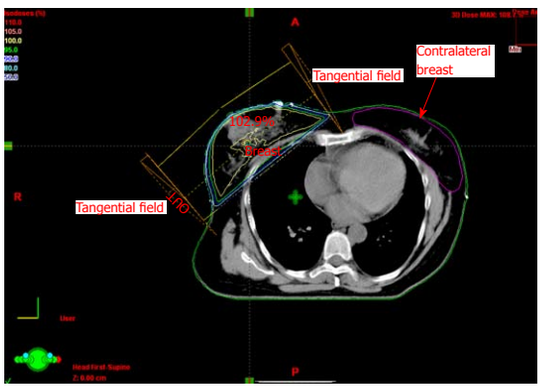

Figure 1 Representative dose distribution for the breast with the contralateral breast contouring.

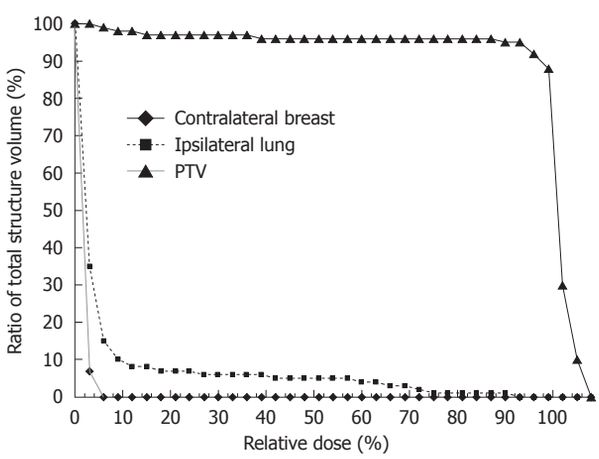

Figure 2 Representative cumulative dose volume histogram.

ment can adversely affect the quality of a patient's life. The drawbacks of a prolonged schedule include inconvenience, loss of earnings and cost of traveling for 5 wk, which can be significant for many women[22]. Shorter schedules, typically delivering a lower total dose in fewer, but larger than 2 Gy fractions, are more convenient for the patients by limiting the number of treatment attendances. Moreover, the reduced resource use in terms of personnel and machine time is advantageous for radiotherapy departments and translates into lower treatment costs. In order to formally validate this therapeutic approach from a societal perspective, however, cost-effectiveness evaluations weighing long-term outcome against the societal costs incurred for many years after treatment are needed[5,6,22]. The efficacy of this schedule has been analyzed by Whelan *et al*[2,3] and seems to be associated with no difference in 10-year LR (6.2% *vs* 6.7%, respectively), DFS, OS, or good/excellent cosmetic outcome (70% *vs* 71%).

In the linear quadratic model, fractionation sensitivity is expressed by the parameter α/β. If α/β is low (e.g., 1 Gy) the tissue is much more sensitive to increasing dose per fraction than if α/β is high (e.g., 10 Gy), while cancerous tissues generally have rather high α/β ratios[20].

After the report of Yarnold *et al*[23] in patients irradiated following breast-conserving surgery with the standard 25 fractions or a 13-fraction radiotherapy scheme, it appears reasonable to use an α/β around 3 Gy in developing fractionation schedules for breast irradiation, which are iso-effective regarding overall late normal tissue effects. Although this study had insufficient statistical power to reliably determine the fractionation sensitivity of breast cancer, tentative results from the trial suggest that the α/β ratios are comparable for both breast fibrosis and local control endpoints. In the past, α/β values of 4-5 Gy have been derived for the radiation response of recurrent or inoperable breast cancer[24,25].

Moreover, an α/β ratio of 4 has been reported for human breast carcinoma cell lines[26-28].

3D-CRT and intensity modulated radiotherapy (IMRT) have allowed more conformal dose distributions to the breast, while selectively sparing surrounding normal tissues. During external beam radiotherapy, the contralateral breast receives radiation due to leakage from the collimator and scatter from primary irradiation[29]. Other factors that contribute to dose may include blocks, orientation of the fields, wedge size, wedge angle and the technique used for treatment[30]. Tangential fields and, if

used, the anterior supraclavicular field contribute to contralateral scatter dose.

The dose to the contralateral breast can be reduced to some extent by reducing the medial wedge angle[30,31]. The closeness of the gantry angle to the contralateral breast is also associated with increase in dose. Contralateral scatter doses are highest for patients with large protruding breasts whose isocentric treatment plan needs the use of a large wedge and higher beam energy[30].

Radiation, especially at sub-therapeutic doses, has been proven to be carcinogenic[32-37]. According to the United Nations Scientific Committee on Effects of Atomic Radiation report[38], experimental exposure of animals to radiation and observations on exposed human populations have shown that ionizing radiations are general carcinogens capable of inducing tumors in almost all tissues of mammals irrespective of species. Dose to the contralateral breast as a result of radiotherapy of breast should not be ignored in radiotherapy, and more so in patients younger than 45 years. The breast tissue is highly sensitive and therefore the contralateral breast must be regarded as an organ at risk (sensitive organ) while planning for radiotherapy. As already reported[32-39], radiotherapy-associated risk of contralateral breast cancer (CBC) increases with decreasing age at first treatment [age < 35 years, hazard ratio (HR) = 1.78, 95% CI: 0.85 to 3.72; age > 45 years, HR = 1.09, 95% CI: 0.82 to 1.45]. This is very important, particularly in women irradiated at a younger age[32-34] and among women treated under the age of 45 years. Boice *et al*[32] have shown that the incidence of radiation-induced breast cancer is a linear function of dose received, with latent periods of over 10 years. Secondary tumors following radiotherapy may be observed around or well outside the margin of the PTV[35-37]. Other important considerations include dose to OARs, including the ipsilateral and contralateral lungs.

Women treated before age 45 years with post-lumpectomy radiotherapy experience 1.5-fold increased risk of CBC compared with those who had post-mastectomy radiotherapy. The joint effects of post-lumpectomy radiotherapy and strong family history for breast cancer on risk of CBC were found to be greater than expected when individual risks were summed (HR = 3.52, 95% CI: 2.07 to 6.02, $P = 0.043$).

Accelerated hypofractionated radiotherapy is currently used because of the similar local control and toxicity rates. To our knowledge, this is the first report on the estimation of the contralateral breast dose using the hypofractionated schedule[3].

Boice *et al*[32] have conducted a case control study in a cohort of 41 109 women diagnosed with breast cancer and analyzed the records. They found mean contralateral breast dose to be 282 cGy with a maximum of 710 cGy and relative overall increase in risk of contralateral breast malignancy due to treatment of primary by radiation to be 1.19. However, the risk of a second malignancy in the contralateral breast was 1.59, significantly high, in patients who underwent radiotherapy at a younger age than 45 years for primary breast malignancy. This indicates high risk for younger patients.

Bhatnagar *et al*[40] reported a comparison of contralateral breast dose during primary breast irradiation using IMRT and conventional tangential field technique. They observed the contralateral breast dose to be 7.74% ± 2.35% of the primary breast dose (5000 cGy) in IMRT treatment planning and 9.74% ± 2.04% of primary breast dose during conventional tangential field technique, i.e. about 20% reduction in contralateral breast dose with IMRT as compared to conventional tangential treatment with wedge. In our study, the measurements are in accordance with the conventional tangential field technique of Bhatnagar *et al*[40].

Tercilla *et al*[41] measured the contralateral breast dose during half beam block and isocentric treatment techniques for patients treated with primary breast irradiation with a Cobalt^{60} unit. They measured contralateral breast dose with thermoluminescent dosimeters (TLD) in 15 patients and the doses were 325-650 cGy during half beam block tangential field treatment and 200-450 cGy without half beam block tangential field treatment for a total primary breast dose of 5040 cGy in 28 equal fractions. They recommended non-use of half beam block techniques; however, this will increase the ipsilateral lung and rib dose[29,42]. Our doses are on the high side as compared to doses reported by Tercilla *et al*[41] because we treated the chest wall using slightly wider fields.

Bhatnagar *et al*[40,43] have studied the effect of breast size on scatter dose to the contralateral breast. They treated 65 patients with breast cancer using 6 MV photon with IMRT technique and measured contralateral breast dose using TLD[44]. The primary breast size volume was calculated by the planning system from CT slices. They found a mean contralateral dose of 7.2% of the primary breast dose (5000 cGy) and found that the contribution to contralateral breast dose is strongly dependent on primary breast size of the patient. Therefore, this has become of more concern in young breast cancer patients with bulky protuberant breasts.

According to Chougule[29], the dose at the contralateral breast nipple was 152.5 to 254.75 cGy for a total primary breast dose of 5000 cGy in 25 equal fractions (Co^{60} fields), which amounted to 3.05%-6.05% of total dose to the diseased breast. Furthermore, it was observed that the maximum contribution to the contralateral breast dose was due to the medical tangential half blocked field. Again in our case, although we used a strictly conformal technique with a full 3-D treatment planning, the measurements are of a higher order than those of Chougule[29], mainly because we did not take measurements only from the nipple where very much less scattered radiation dose is expected, but from the whole contralateral breast and especially from the neighboring breast tissues.

Muller-Runkel *et al*[42] have advocated covering of the contralateral breast with a thin lead sheet to reduce the scattered contribution to contralateral breast skin, though little can be done to reduce the dose from the

lateral tangential field as the dose is caused by internal body scatter.

Using modern techniques of CRT and IMRT, the contralateral breast dose can be reduced by 10%-20% but it still is about 3.05%-6.05% (153-255 Gy) of a primary breast dose of 5000 cGy, which cannot be ignored. IMRT technique provides better dose uniformity as compared to other tangential field techniques, as well as significantly reducing the dose to the contralateral breast[40,43,44].

In a previous study, we have already reported the fine cosmesis in hypofractionated breast irradiation, as used in our institution[45]. In this report we are analyzing the dose at the contralateral breast. Further to ICRU reports[14,15], our results are in accordance with a previous study[30], showing that there are only two significant correlations concerning the contralateral breast volume and the dose. This was logical since the volume of the breast would be expected to be correlated with the incidence of direct or scattered field to be inserted. However, although in previous studies the gantry angle was correlated with higher doses to the contralateral breast[29,30,40,42-44], in our research we have not seen any significant correlation. The reason for this might be the fact that we used a smart immobilization device for the chest wall and the hands, which produces a detachment of the contralateral breast. Moreover, the majority of contralateral breast doses are from the scatter doses coming from the collimator. By using the asymmetric collimator technique, the unwanted scattering doses from the collimator can be minimized. In this current study, asymmetric collimators were used.

In terms of the dose uniformity all over the normal breast tissue (skin included), we did not used field in field techniques or a bolus in order to compensate low skin doses.

The main limitations of the present study are the small number of patients, the absence of *in vivo* dosimetry and the short follow up. Further dosimetric analysis and longer follow up are needed to evaluate the adverse late effects which could be increased because of the hypofractionation schedule used, such as for example, ischemic heart disease, symptomatic rib fracture, symptomatic lung fibrosis. In general, when hypofractionation is used, it is advisable that both possible dose inhomogeneity and normal tissue protection should be taken into account, while the use of three-dimensional conformal techniques should be mandatory[46]. In our clinical routine practice today, further to the use of three-dimensional conformal techniques, we are continuing the study by using *in vivo* dosimetry and further results will be reported after we have evaluated a sufficient number of patients. These results stress the necessity of meticulous patient observation and long follow up to the contralateral breast.

COMMENTS

Background

Lumpectomy followed by breast irradiation is an alternative to mastectomy in early-stage breast cancer. Adjuvant whole breast radiotherapy in patients diagnosed with invasive breast cancer improves local control. Delivering postoperative radiotherapy in a shorter period of time is as effective as longer treatment regimens. Hypofractionated adjuvant radiation schedules have been commonly used in Canada and the United Kingdoms based on data from early invasive breast cancer randomized studies, showing equivalent local control, survival and morbidity rates. Contralateral breast dose from primary breast irradiation has been implicated in the risk of second breast malignancies. The probability of developing contralateral breast cancer represents a serious concern. This study was conducted to measure the dose distribution, related to the treatment planning calculations, in the contralateral mammary gland, when the affected breast was treated with accelerated hypofractionated 3-dimensional conformal radiotherapy.

Research frontiers

The hotspots or important areas in the research field related to the article are as following: (1) The use of dose volume histograms (DVH) for the assessment of the dose to the contralateral breast in a hypofractionated scheme; (2) The usefulness of the 3-dimensional conformal treatment planning technique for the accurate calculation of the dose in the organs at risk, as defined by the radiation oncologist (ipsilateral lung, contralateral breast, *etc.*).

Innovations and breakthroughs

To summarize, this is the first study dealing with the dose to the contralateral breast in a hypofractionated schedule, whereas all similar studies were concerned with the dose in the contralateral breast but under a conventional schedule (2 Gy per fraction instead of 2.66 Gy per fraction). Moreover, for the readers this article incorporates the importance of 3-dimensional treatment planning calculations.

Applications

Further application should be *in-vivo* dosimetry to the contralateral breast together with the modification of the fields (geometry and intensity modulation) for reducing the dose to the contralateral breast. Minimizing the dose to the contralateral breast has to be one of the priorities of the radiation oncologist in short schedules because of the radiosensitivity of this organ at risk. Further study is necessary to assess the long-term clinical impact of this schedule.

Terminology

DVH is the histogram displaying the function between the delivered dose and the volume of a current target or organ. Three-dimensional conformal treatment planning technique concerns the calculation of the dose in each CT plane of the irradiated area. The ICRU defines an organ at risk to be an uninvolved organ that, if given an excess radiation dose, might be damaged and which would compromise the success of the course of radiation therapy. The demonstrable tumor plus the microscopic disease constitute the clinical target volume (CTV). Margins are needed to surround the CTV to ensure that the CTV lies within the treatment field during the entire course of radiation therapy. These internal margins, in addition to the CTV, constitute the internal target volume (ITV). In order to account for setup uncertainties, one adds a setup margin to the ITV to generate a planning target volume.

Peer review

The study seems to be interesting, however there are some points to be reviewed.

REFERENCES

1 **Jabbari S**, Park C, Fowble B. Breast cancer. In: Hansen EK, Mack Roach III, editors. Handbook of evidence-based radiation oncology. 2nd ed. New York: Springer, 2010: 263-305

2 **Whelan T**, MacKenzie R, Julian J, Levine M, Shelley W, Grimard L, Lada B, Lukka H, Perera F, Fyles A, Laukkanen E, Gulavita S, Benk V, Szechtman B. Randomized trial of breast irradiation schedules after lumpectomy for women with lymph node-negative breast cancer. *J Natl Cancer Inst* 2002; **94**: 1143-1150

3 **Whelan TJ**, Pignol JP, Levine MN, Julian JA, MacKenzie R, Parpia S, Shelley W, Grimard L, Bowen J, Lukka H, Perera F, Fyles A, Schneider K, Gulavita S, Freeman C. Long-term results of hypofractionated radiation therapy for breast cancer. *N Engl J Med* 2010; **362**: 513-520

4 **Fujii O**, Hiratsuka J, Nagase N, Tokiya R, Yoden E, Sonoo H, Murashima N, Iha S, Imajyo Y. Whole-breast radiother-

apy with shorter fractionation schedules following breast-conserving surgery: short-term morbidity and preliminary outcomes. *Breast Cancer* 2008; **15**: 86-92
5 **Shelley W**, Brundage M, Hayter C, Paszat L, Zhou S, Mackillop W. A shorter fractionation schedule for postlumpectomy breast cancer patients. *Int J Radiat Oncol Biol Phys* 2000; **47**: 1219-1228
6 **Olivotto IA**, Weir LM, Kim-Sing C, Bajdik CD, Trevisan CH, Doll CM, Lam WY, Basco VE, Jackson SM. Late cosmetic results of short fractionation for breast conservation. *Radiother Oncol* 1996; **41**: 7-13
7 **Yamada Y**, Ackerman I, Franssen E, MacKenzie RG, Thomas G. Does the dose fractionation schedule influence local control of adjuvant radiotherapy for early stage breast cancer? *Int J Radiat Oncol Biol Phys* 1999; **44**: 99-104
8 **Ash DV**, Benson EA, Sainsbury JR, Round C, Head C. Seven-year follow-up on 334 patients treated by breast conserving surgery and short course radical postoperative radiotherapy: a report of the Yorkshire Breast Cancer Group. *Clin Oncol* (R Coll Radiol) 1995; **7**: 93-96
9 **Livi L**, Stefanacci M, Scoccianti S, Dicosmo D, Borghesi S, Nosi F, Simontacchi G, Mangoni M, Paiar F, Ponticelli P, Nori J, Chiavacci A, Biti GP. **Adjuvant hypofractionated** radiation therapy for breast cancer after conserving surgery. *Clin Oncol* (R Coll Radiol) 2007; **19**: 120-124
10 **Koukourakis MI**, Tsoutsou PG, Abatzoglou IM, Sismanidou K, Giatromanolaki A, Sivridis E. Hypofractionated and accelerated radiotherapy with subcutaneous amifostine cytoprotection as short adjuvant regimen after breast-conserving surgery: interim report. *Int J Radiat Oncol Biol Phys* 2009; **74**: 1173-1180
11 **Baillet F**, Housset M, Maylin C, Boisserie G, Bettahar R, Delanian S, Habib F. The use of a specific hypofractionated radiation therapy regimen versus classical fractionation in the treatment of breast cancer: a randomized study of 230 patients. *Int J Radiat Oncol Biol Phys* 1990; **19**: 1131-1133
12 **Bentzen SM**, Agrawal RK, Aird EG, Barrett JM, Barrett-Lee PJ, Bliss JM, Brown J, Dewar JA, Dobbs HJ, Haviland JS, Hoskin PJ, Hopwood P, Lawton PA, Magee BJ, Mills J, Morgan DA, Owen JR, Simmons S, Sumo G, Sydenham MA, Venables K, Yarnold JR. The UK Standardisation of Breast Radiotherapy (START) Trial A of radiotherapy hypofractionation for treatment of early breast cancer: a randomised trial. *Lancet Oncol* 2008; **9**: 331-341
13 **Bentzen SM**, Agrawal RK, Aird EG, Barrett JM, Barrett-Lee PJ, Bentzen SM, Bliss JM, Brown J, Dewar JA, Dobbs HJ, Haviland JS, Hoskin PJ, Hopwood P, Lawton PA, Magee BJ, Mills J, Morgan DA, Owen JR, Simmons S, Sumo G, Sydenham MA, Venables K, Yarnold JR. The UK Standardisation of Breast Radiotherapy (START) Trial B of radiotherapy hypofractionation for treatment of early breast cancer: a randomised trial. *Lancet* 2008; **371**: 1098-1107
14 **International Commission on Radiation Units and Measurements (ICRU)**. Report 50. Prescribing, recording, and reporting photon beam therapy. Bethesda, MD: ICRU, 1993
15 **International Commission on Radiation Units and Measurements (ICRU)**. Report 62. Prescribing, recording, and reporting photon beam therapy (Supplement to ICRU Report 50). Bethesda, MD: ICRU, 1999
16 **Saibishkumar EP**, MacKenzie MA, Severin D, Mihai A, Hanson J, Daly H, Fallone G, Parliament MB, Abdulkarim BS. Skin-sparing radiation using intensity-modulated radiotherapy after conservative surgery in early-stage breast cancer: a planning study. *Int J Radiat Oncol Biol Phys* 2008; **70**: 485-491
17 **Dijkema IM**, Hofman P, Raaijmakers CP, Lagendijk JJ, Battermann JJ, Hillen B. Loco-regional conformal radiotherapy of the breast: delineation of the regional lymph node clinical target volumes in treatment position. *Radiother Oncol* 2004; **71**: 287-295
18 **Hiatt JR**, Evans SB, Price LL, Cardarelli GA, Dipetrillo TA, Wazer DE. Dose-modeling study to compare external beam techniques from protocol NSABP B-39/RTOG 0413 for patients with highly unfavorable cardiac anatomy. *Int J Radiat Oncol Biol Phys* 2006; **65**: 1368-1374
19 **Williamson D**, Dinniwell R, Fung S, Pintilie M, Done SJ, Fyles AW. Local control with conventional and hypofractionated adjuvant radiotherapy after breast-conserving surgery for ductal carcinoma in-situ. *Radiother Oncol* 2010; **95**: 317-320
20 **Kurtz JM**. The clinical radiobiology of breast cancer radiotherapy. *Radiother Oncol* 2005; **75**: 6-8
21 **Cox JD**, Stetz J, Pajak TF. Toxicity criteria of the Radiation Therapy Oncology Group (RTOG) and the European Organization for Research and Treatment of Cancer (EORTC) *Int J Radiat Oncol Biol Phys* 1995; **31**: 1341-1346
22 **Lievens Y**. Hypofractionated breast radiotherapy: financial and economic consequences. *Breast* 2010; **19**: 192-197
23 **Yarnold J**, Ashton A, Bliss J, Homewood J, Harper C, Hanson J, Haviland J, Bentzen S, Owen R. Fractionation sensitivity and dose response of late adverse effects in the breast after radiotherapy for early breast cancer: long-term results of a randomised trial. *Radiother Oncol* 2005; **75**: 9-17
24 **COHEN L**. Radiotherapy in breast cancer. I. The dose-time relationship theoretical considerations. *Br J Radiol* 1952; **25**: 636-642
25 **Douglas BG**, Castro JR. Novel fractionation schemes and high linear energy transfer. *Prog Exp Tumor Res* 1984; **28**: 152-165
26 **Williams MV**, Denekamp J, Fowler JF. **A review of alpha/** beta ratios for experimental tumors: implications for clinical studies of altered fractionation. *Int J Radiat Oncol Biol Phys* 1985; **11**: 87-96
27 **Matthews JH**, Meeker BE, Chapman JD. Response of human tumor cell lines in vitro to fractionated irradiation. *Int J Radiat Oncol Biol Phys* 1989; **16**: 133-138
28 **Joiner MC**, Bentzen SM. Time-dose relationships: the linear-quadratic approach. In: Steel GG, editor. Basic clinical radiobiology. London: Arnold, 2002: 120-133
29 **Chougule A**. Radiation dose to contralateral breast during treatment of breast malignancy by radiotherapy. *J Cancer Res Ther* 2007; **3**: 8-11
30 **Fraass BA**, Roberson PL, Lichter AS. Dose to the contralateral breast due to primary breast irradiation. *Int J Radiat Oncol Biol Phys* 1985; **11**: 485-497
31 **Brooks PS**. Dose to contralateral breast--a comparative study. *Med Dosim* 1995; **20**: 301-307
32 **Boice JD**, Harvey EB, Blettner M, Stovall M, Flannery JT. Cancer in the contralateral breast after radiotherapy for breast cancer. *N Engl J Med* 1992; **326**: 781-785
33 **Gao X**, Fisher SG, Emami B. Risk of second primary cancer in the contralateral breast in women treated for early-stage breast cancer: a population-based study. *Int J Radiat Oncol Biol Phys* 2003; **56**: 1038-1045
34 **Unnithan J**, Macklis RM. Contralateral breast cancer risk. *Radiother Oncol* 2001; **60**: 239-246
35 **Dörr W**, Herrmann T. Second primary tumors after radiotherapy for malignancies. Treatment-related parameters. *Strahlenther Onkol* 2002; **178**: 357-362
36 **Boice JD**, Engholm G, Kleinerman RA, Blettner M, Stovall M, Lisco H, Moloney WC, Austin DF, Bosch A, Cookfair DL. Radiation dose and second cancer risk in patients treated for cancer of the cervix. *Radiat Res* 1988; **116**: 3-55
37 **Brenner DJ**, Curtis RE, Hall EJ, Ron E. Second malignancies in prostate carcinoma patients after radiotherapy compared with surgery. *Cancer* 2000; **88**: 398-406
38 **United Nations Scientific Committee on the Effects of Atomic Radiation**. Sources and effects of ionizing radiation. New York, NY: United Nations, 1977
39 **Hooning MJ**, Aleman BM, Hauptmann M, Baaijens MH,

Klijn JG, Noyon R, Stovall M, van Leeuwen FE. Roles of radiotherapy and chemotherapy in the development of contralateral breast cancer. *J Clin Oncol* 2008; **26**: 5561-5568

40 **Bhatnagar AK**, Heron DE, Deutsch M, Brandner E, Wu A, Kalnicki S. Does breast size affect the scatter dose to the ipsilateral lung, heart, or contralateral breast in primary breast irradiation using intensity-modulated radiation therapy (IMRT)? *Am J Clin Oncol* 2006; **29**: 80-84

41 **Tercilla O**, Krasin F, Lawn-Tsao L. Comparison of contralateral breast doses from 1/2 beam block and isocentric treatment techniques for patients treated with primary breast irradiation with 60CO. *Int J Radiat Oncol Biol Phys* 1989; **17**: 205-210

42 **Muller-Runkel R**, Kalokhe UP. Method for reducing scatter radiation dose to the contralateral breast during tangential breast irradiation therapy. *Radiology* 1994; **191**: 853-855

43 **Bhatnagar AK**, Brandner E, Sonnik D, Wu A, Kalnicki S, Deutsch M, Heron DE. Intensity modulated radiation therapy (IMRT) reduces the dose to the contralateral breast when compared to conventional tangential fields for primary breast irradiation. *Breast Cancer Res Treat* 2006; **96**: 41-46

44 **Bhatnagar AK**, Brandner E, Sonnik D, Wu A, Kalnicki S, Deutsch M, Heron DE. Intensity-modulated radiation therapy (IMRT) reduces the dose to the contralateral breast when compared to conventional tangential fields for primary breast irradiation: initial report. *Cancer J* 2004; **10**: 381-385

45 **Zygogianni AG**, Kouvaris JR, Kouloulias V, Armpilia C, Antypas C, Vlachos L. Hypofractionated accelerated irradiation for stage I-II breast carcinoma: a phase II study. *Breast J* 2010; **16**: 337-338

46 **Plataniotis G**. Hypofractionated radiotherapy in the treatment of early breast cancer. *World J Radiol* 2010; **2**: 197-202

S- Editor Cheng JX **L- Editor** Logan S **E- Editor** Zheng XM

World Journal of Radiology

Online Submissions: http://www.wjgnet.com/1949-8470office
wjr@wjgnet.com
www.wjgnet.com

World J Radiol 2011 September 28; 3(9): I
ISSN 1949-8470 (online)

Acknowledgments to reviewers of *World Journal of Radiology*

Many reviewers have contributed their expertise and time to the peer review, a critical process to ensure the quality of *World Journal of Radiology*. The editors and authors of the articles submitted to the journal are grateful to the following reviewers for evaluating the articles (including those published in this issue and those rejected for this issue) during the last editing time period.

Sandip Basu, MBBS (Hons), DRM, DNB, MNAMS, Head, Nuclear Medicine Academic Programme, Radiation Medicine Centre, Bhabha Atomic Research Centre, Tata Memorial Hospital Annexe, Parel, Bombay 400012, India

Ragab Hani Donkol, Professor, Radiology Department, Aseer Central Hospital, 34 Abha, Saudi Arabia

Cem Onal, MD, Department of Radiation Oncology, Adana Research and Treatment Centre, Baskent University Medical Faculty, 01120 Yuregir, Adana, Turkey

Frank Pilleul, MD, PhD, Professor, Department of Radiology, Hospices Civils de Lyon, CHU E. Herriot, Pavillon H, Department of Gastrointestinal Imaging, Place Arsonval, 69003 Lyon, Cedex, France

Sudsriluk Sampatchalit, MD, Lieutenant Colonel, Radiology, Phramongutglao Royal Thai Army Hospital, 315 Ratchawithi Road, Ratchathewi, Bangkok 10400, Thailand

Wenbao Wang, MD, Orthopaedic Department, Columbia University Medical Center, 106 Fort Washington Avenue, Apt 3H, New York, NY 10032, United States

WJR World Journal of Radiology

Online Submissions: http://www.wjgnet.com/1949-8470office
wjr@wjgnet.com
www.wjgnet.com

World J Radiol 2011 September 28; 3(9): I
ISSN 1949-8470 (online)

Events Calendar 2011

January 23-27
Radiology at Snowbird
San Diego, Mexico

January 24-28
Neuro/ENT at the Beach
Palm Beach, FL, United States

February 28-29
MIAD 2011 - 2nd International Workshop on Medical Image Analysis and Description for Diagnosis System
Rome, Italy

February 5-6
Washington Neuroradiology Review
Arlington, VA, United States

February 12-17
MI11 - SPIE Medical Imaging 2011
Lake Buena Vista, FL, United States

February 17-18
2nd National Conference Diagnostic and Interventional Radiology 2011
London, United Kingdom

Februrary 17-18
VII National Neuroradiology Course
Lleida, Spain

February 18
Radiology in child protection
Nottingham, United Kingdom

Februrary 19-22
COMPREHENSIVE REVIEW OF MUSCULOSKELETAL MRI
Lake Buena Vista, FL, United States

March 2-5
2011 Abdominal Radiology Course
Carlsbad, CA, United States

March 3-7
European Congress of Radiology Meeting ECR 2011 Vienna, Austria

March 6-9
World Congress Thoracic Imaging - IV
Bonita Springs, FL, United States

March 14-18
9th Annual NYU Radiology Alpine Imaging Symposium at Beaver Creek
Beaver Creek, CO, United States

March 20-25
Abdominal Radiology Course 2011
Carlsbad, CA, United States

March 26-31
2011 SIR Annual Meeting
Chicago, IL, United States

March 28-April 1
University of Utah Neuroradiology 2nd Intensive Interactive Brain & Spine Imaging Conference
Salt Lake City, UT, United States

April 3-8
1st Annual Ottawa Radiology Resident Review
Ottawa, Canada

April 3-8
43rd International Diagnostic Course Davos on Diagnostic Imaging and Interventional Techniques
Davos, Switzerland

April 6-9
Image-Based Neurodiagnosis: Intensive Clinical and Radiologic Review, CAQ Preparation
Cincinnati, OH, United States

April 28-May 1
74th Annual Scientific Meeting of the Canadian Association of Radiologists CAR
Montreal, Canada

May 5-8
EMBL Conference-Sixth International Congress on Electron Tomography
Heidelberg, Germany

May 10-13
27th Iranian Congress of Radiology
Tehran, Iran

May 14-21
Radiology in Marrakech
Marrakech, Morocco

May 21-24
European Society of Gastrointestinal and Abdominal Radiology 2011 Annual Meeting
Venice, Italy

May 23-25
Sports Medicine Imaging State of the Art: A Collaborative Course for Radiologists and Sports Medicine Specialists
New York, NY, United States

May 24-26
Russian Congress of Radiology
Moscow, Russia

May 28-31
International Congress of Pediatric Radiology (IPR)
London, United Kingdom

June 4-8
58th Annual Meeting of the Society of Nuclear Medicine
San Antonio, TX, United States

June 6-8
UKRC 2011 - UK Radiological Congress
Manchester, United Kingdom

June 8-11
CIRA 2011 - Canadian Internventinal Radiology Association Meeting
Montreal, QC, Canada

June 9-10
8th ESGAR Liver Imaging Workshop
Dublin, Ireland

June 17-19
ASCI 2011 - 5th Congress of Asian Society of Cardiovascular Imaging
Hong Kong, China

June 22-25
CARS 2011 - Computer Assisted Radiology and Surgery - 25th International Congress and Exhibition Berlin, Germany

June 27-July 1
NYU Summer Radiology Symposium at The Sagamore
Lake George, NY, United States

July 18-22
Clinical Case-Based Radiology Update in Iceland
Reykjavik, Iceland

August 1-5
NYU Clinical Imaging Symposium in Santa Fe
Santa Fe, NM, United States

September 22-25
European Society of Neuroradiology (ESNR) XXXV Congress and 19th Advanced Course
Antwerp, Belgium

October 12-14
International Conference Vipimage 2011 - Computational Vision and Medical Image Processing
Algarve, Portugal

October 15-16
Essentials of Emergency and Trauma Radiology
Ottawa, Canada

October 23-29
2011 IEEE NSS - 2011 IEEE Nuclear Science Symposium and Medical Imaging Conference
Valencia, Spain

October 25-28
NYU Radiology in Scottsdale - Fall Radiology Symposium in Scottsdale
Scottsdale, AZ, United States

October 28-30
Fourth National Congress of Professionals of Radiological Techniques Florianópolis, Brazil

October 28-30
Multi-Modality Gynecological & Obstetric Imaging
Ottawa, Canada

November 3-4
9th ESGAR Liver Imaging Workshop
Taormina, Italy

November 15-19
EANM 2011 - Annual Congress of the European Association of Nuclear Medicine
Birmingham, United Kingdom

November 22-29
NSS/MIC - Nuclear Science Symposium and Medical Imaging Conference 2011 Valencia, Spain

November 26-28
8th Asia Oceaninan Congress of Neuro-Radiology Bangkok, Thailand

World Journal of Radiology

Online Submissions: http://www.wjgnet.com/1949-8470office
wjr@wjgnet.com
www.wjgnet.com

World J Radiol 2011 September 28; 3(9): I-V
ISSN 1949-8470 (online)

INSTRUCTIONS TO AUTHORS

GENERAL INFORMATION

World Journal of Radiology (*World J Radiol*, *WJR*, online ISSN 1949-8470, DOI: 10.4329), is a monthly, open-access (OA), peer-reviewed journal supported by an editorial board of 319 experts in Radiology from 40 countries.

The biggest advantage of the OA model is that it provides free, full-text articles in PDF and other formats for experts and the public without registration, which eliminates the obstacle that traditional journals possess and usually delays the speed of the propagation and communication of scientific research results. The open access model has been proven to be a true approach that may achieve the ultimate goal of the journals, i.e. the maximization of the value to the readers, authors and society.

Maximization of personal benefits

The role of academic journals is to exhibit the scientific levels of a country, a university, a center, a department, and even a scientist, and build an important bridge for communication between scientists and the public. As we all know, the significance of the publication of scientific articles lies not only in disseminating and communicating innovative scientific achievements and academic views, as well as promoting the application of scientific achievements, but also in formally recognizing the "priority" and "copyright" of innovative achievements published, as well as evaluating research performance and academic levels. So, to realize these desired attributes of *WJR* and create a well-recognized journal, the following four types of personal benefits should be maximized. The maximization of personal benefits refers to the pursuit of the maximum personal benefits in a well-considered optimal manner without violation of the laws, ethical rules and the benefits of others. (1) Maximization of the benefits of editorial board members: The primary task of editorial board members is to give a peer review of an unpublished scientific article via online office system to evaluate its innovativeness, scientific and practical values and determine whether it should be published or not. During peer review, editorial board members can also obtain cutting-edge information in that field at first hand. As leaders in their field, they have priority to be invited to write articles and publish commentary articles. We will put peer reviewers' names and affiliations along with the article they reviewed in the journal to acknowledge their contribution; (2) Maximization of the benefits of authors: Since *WJR* is an open-access journal, readers around the world can immediately download and read, free of charge, high-quality, peer-reviewed articles from *WJR* official website, thereby realizing the goals and significance of the communication between authors and peers as well as public reading; (3) Maximization of the benefits of readers: Readers can read or use, free of charge, high-quality peer-reviewed articles without any limits, and cite the arguments, viewpoints, concepts, theories, methods, results, conclusion or facts and data of pertinent literature so as to validate the innovativeness, scientific and practical values of their own research achievements, thus ensuring that their articles have novel arguments or viewpoints, solid evidence and correct conclusion; and (4) Maximization of the benefits of employees: It is an iron law that a first-class journal is unable to exist without first-class editors, and only first-class editors can create a first-class academic journal. We insist on strengthening our team cultivation and construction so that every employee, in an open, fair and transparent environment, could contribute their wisdom to edit and publish high-quality articles, thereby realizing the maximization of the personal benefits of editorial board members, authors and readers, and yielding the greatest social and economic benefits.

Aims and scope

The major task of *WJR* is to rapidly report the most recent improvement in the research of medical imaging and radiation therapy by the radiologists. *WJR* accepts papers on the following aspects related to radiology: Abdominal radiology, women health radiology, cardiovascular radiology, chest radiology, genitourinary radiology, neuroradiology, head and neck radiology, interventional radiology, musculoskeletal radiology, molecular imaging, pediatric radiology, experimental radiology, radiological technology, nuclear medicine, PACS and radiology informatics, and ultrasound. We also encourage papers that cover all other areas of radiology as well as basic research.

Columns

The columns in the issues of *WJR* will include: (1) Editorial: To introduce and comment on major advances and developments in the field; (2) Frontier: To review representative achievements, comment on the state of current research, and propose directions for future research; (3) Topic Highlight: This column consists of three formats, including (A) 10 invited review articles on a hot topic, (B) a commentary on common issues of this hot topic, and (C) a commentary on the 10 individual articles; (4) Observation: To update the development of old and new questions, highlight unsolved problems, and provide strategies on how to solve the questions; (5) Guidelines for Basic Research: To provide guidelines for basic research; (6) Guidelines for Clinical Practice: To provide guidelines for clinical diagnosis and treatment; (7) Review: To review systemically progress and unresolved problems in the field, comment on the state of current research, and make suggestions for future work; (8) Original Articles: To report innovative and original findings in radiology; (9) Brief Articles: To briefly report the novel and innovative findings in radiology; (10) Case Report: To report a rare or typical case; (11) Letters to the Editor: To discuss and make reply to the contributions published in *WJR*, or to introduce and comment on a controversial issue of general interest; (12) Book Reviews: To introduce and comment on quality monographs of radiology; and (13) Guidelines: To introduce consensuses and guidelines reached by international and national academic authorities worldwide on the research in radiology.

Name of journal

World Journal of Radiology

ISSN

ISSN 1949-8470 (online)

Indexed and Abstracted in

PubMed Central, PubMed, Digital Object Identifer, and Directory of Open Access Journals.

Published by

Baishideng Publishing Group Co., Limited.

SPECIAL STATEMENT

All articles published in this journal represent the viewpoints of the authors except where indicated otherwise.

Biostatistical editing

Statisital review is performed after peer review. We invite an expert in Biomedical Statistics from to evaluate the statistical method used in the paper, including *t*-test (group or paired comparisons), chi-squared test, Ridit, probit, logit, regression (linear, curvilinear, or stepwise), correlation, analysis of variance, analysis of covariance, *etc*. The reviewing points include: (1) Statistical methods should be described when they are used to verify the results; (2) Whether the statistical techniques are suitable or correct; (3) Only homogeneous data can be averaged. Standard deviations are preferred to standard errors. Give the number of observations and subjects (*n*). Losses in observations, such as drop-outs from the study should be reported; (4) Values such as ED50, LD50, IC50 should have their 95% confidence limits calculated and compared by weighted probit analysis (Bliss and Finney); and (5) The word 'significantly' should be replaced by its synonyms (if it indicates extent) or the *P* value (if it indicates statistical significance).

Conflict-of-interest statement

In the interests of transparency and to help reviewers assess any potential bias, *WJR* requires authors of all papers to declare any competing commercial, personal, political, intellectual, or religious interests in relation to the submitted work. Referees are also asked to indicate any potential conflict they might have reviewing a particular paper. Before submitting, authors are suggested to read "Uniform Requirements for Manuscripts Submitted to Biomedical Journals: Ethical Considerations in the Conduct and Reporting of Research: Conflicts of Interest" from International Committee of Medical Journal Editors (ICMJE), which is available at: http://www.icmje.org/ethical_4conflicts.html.

Sample wording: [Name of individual] has received fees for serving as a speaker, a consultant and an advisory board member for [names of organizations], and has received research funding from [names of organization]. [Name of individual] is an employee of [name of organization]. [Name of individual] owns stocks and shares in [name of organization]. [Name of individual] owns patent [patent identification and brief description].

Statement of informed consent

Manuscripts should contain a statement to the effect that all human studies have been reviewed by the appropriate ethics committee or it should be stated clearly in the text that all persons gave their informed consent prior to their inclusion in the study. Details that might disclose the identity of the subjects under study should be omitted. Authors should also draw attention to the Code of Ethics of the World Medical Association (Declaration of Helsinki, 1964, as revised in 2004).

Statement of human and animal rights

When reporting the results from experiments, authors should follow the highest standards and the trial should conform to Good Clinical Practice (for example, US Food and Drug Administration Good Clinical Practice in FDA-Regulated Clinical Trials; UK Medicines Research Council Guidelines for Good Clinical Practice in Clinical Trials) and/or the World Medical Association Declaration of Helsinki. Generally, we suggest authors follow the lead investigator's national standard. If doubt exists whether the research was conducted in accordance with the above standards, the authors must explain the rationale for their approach and demonstrate that the institutional review body explicitly approved the doubtful aspects of the study.

Before submitting, authors should make their study approved by the relevant research ethics committee or institutional review board. If human participants were involved, manuscripts must be accompanied by a statement that the experiments were undertaken with the understanding and appropriate informed consent of each. Any personal item or information will not be published without explicit consents from the involved patients. If experimental animals were used, the materials and methods (experimental procedures) section must clearly indicate that appropriate measures were taken to minimize pain or discomfort, and details of animal care should be provided.

SUBMISSION OF MANUSCRIPTS

Manuscripts should be typed in 1.5 line spacing and 12 pt. Book Antiqua with ample margins. Number all pages consecutively, and start each of the following sections on a new page: Title Page, Abstract, Introduction, Materials and Methods, Results, Discussion, Acknowledgements, References, Tables, Figures, and Figure Legends. Neither the editors nor the publisher are responsible for the opinions expressed by contributors. Manuscripts formally accepted for publication become the permanent property of Baishideng Publishing Group Co., Limited, and may not be reproduced by any means, in whole or in part, without the written permission of both the authors and the publisher. We reserve the right to copy-edit and put onto our website accepted manuscripts. Authors should follow the relevant guidelines for the care and use of laboratory animals of their institution or national animal welfare committee. For the sake of transparency in regard to the performance and reporting of clinical trials, we endorse the policy of the ICMJE to refuse to publish papers on clinical trial results if the trial was not recorded in a publicly-accessible registry at its outset. The only register now available, to our knowledge, is http://www.clinicaltrials.gov sponsored by the United States National Library of Medicine and we encourage all potential contributors to register with it. However, in the case that other registers become available you will be duly notified. A letter of recommendation from each author's organization should be provided with the contributed article to ensure the privacy and secrecy of research is protected.

Authors should retain one copy of the text, tables, photographs and illustrations because rejected manuscripts will not be returned to the author(s) and the editors will not be responsible for loss or damage to photographs and illustrations sustained during mailing.

Online submissions

Manuscripts should be submitted through the Online Submission System at: http://www.wjgnet.com/1949-8470office. Authors are highly recommended to consult the ONLINE INSTRUCTIONS TO AUTHORS (http://www.wjgnet.com/1949-8470/g_info_20100316162358.htm) before attempting to submit online. For assistance, authors encountering problems with the Online Submission System may send an email describing the problem to wjr@wjgnet.com, or by telephone: +86-10-85381892. If you submit your manuscript online, do not make a postal contribution. Repeated online submission for the same manuscript is strictly prohibited.

MANUSCRIPT PREPARATION

All contributions should be written in English. All articles must be submitted using word-processing software. All submissions must be typed in 1.5 line spacing and 12 pt. Book Antiqua with ample margins. Style should conform to our house format. Required information for each of the manuscript sections is as follows:

Title page

Title: Title should be less than 12 words.

Running title: A short running title of less than 6 words should be provided.

Authorship: Authorship credit should be in accordance with the standard proposed by International Committee of Medical Journal Editors, based on (1) substantial contributions to conception and design, acquisition of data, or analysis and interpretation of data; (2) drafting the article or revising it critically for important intellectual content; and (3) final approval of the version to be published. Authors should meet conditions 1, 2, and 3.

Institution: Author names should be given first, then the complete name of institution, city, province and postcode. For example, Xu-Chen Zhang, Li-Xin Mei, Department of Pathology, Chengde Medical College, Chengde 067000, Hebei Province, China. One author may be represented from two institutions, for example, George Sgourakis, Department of General, Visceral, and Transplantation Surgery, Essen 45122, Germany; George Sgourakis, 2nd Surgical

Department, Korgialenio-Benakio Red Cross Hospital, Athens 15451, Greece

Author contributions: The format of this section should be: Author contributions: Wang CL and Liang L contributed equally to this work; Wang CL, Liang L, Fu JF, Zou CC, Hong F and Wu XM designed the research; Wang CL, Zou CC, Hong F and Wu XM performed the research; Xue JZ and Lu JR contributed new reagents/analytic tools; Wang CL, Liang L and Fu JF analyzed the data; and Wang CL, Liang L and Fu JF wrote the paper.

Supportive foundations: The complete name and number of supportive foundations should be provided, e.g., Supported by National Natural Science Foundation of China, No. 30224801

Correspondence to: Only one corresponding address should be provided. Author names should be given first, then author title, affiliation, the complete name of institution, city, postcode, province, country, and email. All the letters in the email should be in lower case. A space interval should be inserted between country name and email address. For example, Montgomery Bissell, MD, Professor of Medicine, Chief, Liver Center, Gastroenterology Division, University of California, Box 0538, San Francisco, CA 94143, United States. montgomery.bissell@ucsf.edu

Telephone and fax: Telephone and fax should consist of +, country number, district number and telephone or fax number, e.g., Telephone: +86-10-85381892 Fax: +86-10-85381893

Peer reviewers: All articles received are subject to peer review. Normally, three experts are invited for each article. Decision for acceptance is made only when at least two experts recommend an article for publication. Reviewers for accepted manuscripts are acknowledged in each manuscript, and reviewers of articles which were not accepted will be acknowledged at the end of each issue. To ensure the quality of the articles published in *WJR*, reviewers of accepted manuscripts will be announced by publishing the name, title/position and institution of the reviewer in the footnote accompanying the printed article. For example, reviewers: Professor Jing-Yuan Fang, Shanghai Institute of Digestive Disease, Shanghai, Affiliated Renji Hospital, Medical Faculty, Shanghai Jiaotong University, Shanghai, China; Professor Xin-Wei Han, Department of Radiology, The First Affiliated Hospital, Zhengzhou University, Zhengzhou, Henan Province, China; and Professor Anren Kuang, Department of Nuclear Medicine, Huaxi Hospital, Sichuan University, Chengdu, Sichuan Province, China.

Abstract

There are unstructured abstracts (no more than 256 words) and structured abstracts (no more than 480). The specific requirements for structured abstracts are as follows:

An informative, structured abstracts of no more than 480 words should accompany each manuscript. Abstracts for original contributions should be structured into the following sections. AIM (no more than 20 words): Only the purpose should be included. Please write the aim as the form of "To investigate/study/…; MATERIALS AND METHODS (no more than 140 words); RESULTS (no more than 294 words): You should present *P* values where appropriate and must provide relevant data to illustrate how they were obtained, e.g. 6.92 ± 3.86 *vs* 3.61 ± 1.67, $P < 0.001$; CONCLUSION (no more than 26 words).

Key words

Please list 5-10 key words, selected mainly from *Index Medicus*, which reflect the content of the study.

Text

For articles of these sections, original articles and brief articles, the main text should be structured into the following sections: INTRODUCTION, MATERIALS AND METHODS, RESULTS and DISCUSSION, and should include appropriate Figures and Tables. Data should be presented in the main text or in Figures and Tables, but not in both. The main text format of these sections, editorial, topic highlight, case report, letters to the editors, can be found at: http://www.wjgnet.com/1949-8470/g_info_20100313183720.htm.

Illustrations

Figures should be numbered as 1, 2, 3, *etc.*, and mentioned clearly in the main text. Provide a brief title for each figure on a separate page. Detailed legends should not be provided under the figures. This part should be added into the text where the figures are applicable. Figures should be either Photoshop or Illustrator files (in tiff, eps, jpeg formats) at high-resolution. Examples can be found at: http://www.wjgnet.com/1007-9327/13/4520.pdf; http://www.wjgnet.com/1007-9327/13/4554.pdf; http://www.wjgnet.com/1007-9327/13/4891.pdf; http://www.wjgnet.com/1007-9327/13/4986.pdf; http://www.wjgnet.com/1007-9327/13/4498.pdf. Keeping all elements compiled is necessary in line-art image. Scale bars should be used rather than magnification factors, with the length of the bar defined in the legend rather than on the bar itself. File names should identify the figure and panel. Avoid layering type directly over shaded or textured areas. Please use uniform legends for the same subjects. For example: Figure 1 Pathological changes in atrophic gastritis after treatment. A: ...; B: ...; C: ...; D: ...; E: ...; F: ...; G: …*etc.* It is our principle to publish high resolution-figures for the printed and E-versions.

Tables

Three-line tables should be numbered 1, 2, 3, *etc.*, and mentioned clearly in the main text. Provide a brief title for each table. Detailed legends should not be included under tables, but rather added into the text where applicable. The information should complement, but not duplicate the text. Use one horizontal line under the title, a second under column heads, and a third below the Table, above any footnotes. Vertical and italic lines should be omitted.

Notes in tables and illustrations

Data that are not statistically significant should not be noted. $^{a}P < 0.05$, $^{b}P < 0.01$ should be noted ($P > 0.05$ should not be noted). If there are other series of *P* values, $^{c}P < 0.05$ and $^{d}P < 0.01$ are used. A third series of *P* values can be expressed as $^{e}P < 0.05$ and $^{f}P < 0.01$. Other notes in tables or under illustrations should be expressed as ^{1}F, ^{2}F, ^{3}F; or sometimes as other symbols with a superscript (Arabic numerals) in the upper left corner. In a multi-curve illustration, each curve should be labeled with ●, ○, ■, □, ▲, △, *etc.*, in a certain sequence.

Acknowledgments

Brief acknowledgments of persons who have made genuine contributions to the manuscript and who endorse the data and conclusions should be included. Authors are responsible for obtaining written permission to use any copyrighted text and/or illustrations.

REFERENCES

Coding system

The author should number the references in Arabic numerals according to the citation order in the text. Put reference numbers in square brackets in superscript at the end of citation content or after the cited author's name. For citation content which is part of the narration, the coding number and square brackets should be typeset normally. For example, "Crohn's disease (CD) is associated with increased intestinal permeability[1,2]". If references are cited directly in the text, they should be put together within the text, for example, "From references[19,22-24], we know that..."

When the authors write the references, please ensure that the order in text is the same as in the references section, and also ensure the spelling accuracy of the first author's name. Do not list the same citation twice.

PMID and DOI

Pleased provide PubMed citation numbers to the reference list, e.g. PMID and DOI, which can be found at http://www.ncbi.nlm.nih.gov/sites/entrez?db=pubmed and http://www.crossref.org/SimpleTextQuery/, respectively. The numbers will be used in E-version of this journal.

Style for journal references

Authors: the name of the first author should be typed in bold-faced letters. The family name of all authors should be typed with the initial letter capitalized, followed by their abbreviated first and middle initials. (For example, Lian-Sheng Ma is abbreviated as Ma LS, Bo-Rong Pan as Pan BR). The title of the cited article and italicized journal title (journal title should be in its abbreviated form as shown in PubMed), publication date, volume number (in black), start page, and end page [PMID: 11819634 DOI: 10.3748/wjg.13.5396].

Style for book references

Authors: the name of the first author should be typed in bold-faced letters. The surname of all authors should be typed with the initial letter capitalized, followed by their abbreviated middle and first initials. (For example, Lian-Sheng Ma is abbreviated as Ma LS, Bo-Rong Pan as Pan BR) Book title. Publication number. Publication place: Publication press, Year: start page and end page.

Format

Journals

English journal article (list all authors and include the PMID where applicable)

1 **Jung EM**, Clevert DA, Schreyer AG, Schmitt S, Rennert J, Kubale R, Feuerbach S, Jung F. Evaluation of quantitative contrast harmonic imaging to assess malignancy of liver tumors: A prospective controlled two-center study. *World J Gastroenterol* 2007; **13**: 6356-6364 [PMID: 18081224 DOI: 10.3748/wjg.13.6356]

Chinese journal article (list all authors and include the PMID where applicable)

2 **Lin GZ**, Wang XZ, Wang P, Lin J, Yang FD. Immunologic effect of Jianpi Yishen decoction in treatment of Pixu-diarrhoea. *Shijie Huaren Xiaohua Zazhi* 1999; **7**: 285-287

In press

3 **Tian D**, Araki H, Stahl E, Bergelson J, Kreitman M. Signature of balancing selection in Arabidopsis. *Proc Natl Acad Sci USA* 2006; In press

Organization as author

4 **Diabetes Prevention Program Research Group**. Hypertension, insulin, and proinsulin in participants with impaired glucose tolerance. *Hypertension* 2002; **40**: 679-686 [PMID: 12411462 PMCID:2516377 DOI:10.1161/01.HYP.0000035706.28494.09]

Both personal authors and an organization as author

5 **Vallancien G**, Emberton M, Harving N, van Moorselaar RJ; Alf-One Study Group. Sexual dysfunction in 1, 274 European men suffering from lower urinary tract symptoms. *J Urol* 2003; **169**: 2257-2261 [PMID: 12771764 DOI:10.1097/01.ju.0000067940.76090.73]

No author given

6 21st century heart solution may have a sting in the tail. *BMJ* 2002; **325**: 184 [PMID: 12142303 DOI:10.1136/bmj.325.7357.184]

Volume with supplement

7 **Geraud G**, Spierings EL, Keywood C. Tolerability and safety of frovatriptan with short- and long-term use for treatment of migraine and in comparison with sumatriptan. *Headache* 2002; **42** Suppl 2: S93-99 [PMID: 12028325 DOI:10.1046/j.1526-4610.42.s2.7.x]

Issue with no volume

8 **Banit DM**, Kaufer H, Hartford JM. Intraoperative frozen section analysis in revision total joint arthroplasty. *Clin Orthop Relat Res* 2002; (**401**): 230-238 [PMID: 12151900 DOI:10.1097/00003086-200208000-00026]

No volume or issue

9 Outreach: Bringing HIV-positive individuals into care. *HRSA Careaction* 2002; 1-6 [PMID: 12154804]

Books

Personal author(s)

10 **Sherlock S**, Dooley J. Diseases of the liver and billiary system. 9th ed. Oxford: Blackwell Sci Pub, 1993: 258-296

Chapter in a book (list all authors)

11 **Lam SK**. Academic investigator's perspectives of medical treatment for peptic ulcer. In: Swabb EA, Azabo S. Ulcer disease: investigation and basis for therapy. New York: Marcel Dekker, 1991: 431-450

Author(s) and editor(s)

12 **Breedlove GK**, Schorfheide AM. Adolescent pregnancy. 2nd ed. Wieczorek RR, editor. White Plains (NY): March of Dimes Education Services, 2001: 20-34

Conference proceedings

13 **Harnden P**, Joffe JK, Jones WG, editors. Germ cell tumours V. Proceedings of the 5th Germ cell tumours Conference; 2001 Sep 13-15; Leeds, UK. New York: Springer, 2002: 30-56

Conference paper

14 **Christensen S**, Oppacher F. An analysis of Koza's computational effort statistic for genetic programming. In: Foster JA, Lutton E, Miller J, Ryan C, Tettamanzi AG, editors. Genetic programming. EuroGP 2002: Proceedings of the 5th European Conference on Genetic Programming; 2002 Apr 3-5; Kinsdale, Ireland. Berlin: Springer, 2002: 182-191

Electronic journal (list all authors)

15 Morse SS. Factors in the emergence of infectious diseases. Emerg Infect Dis serial online, 1995-01-03, cited 1996-06-05; 1(1): 24 screens. Available from: URL: http://www.cdc.gov/ncidod/eid/index.htm

Patent (list all authors)

16 **Pagedas AC**, inventor; Ancel Surgical R&D Inc., assignee. Flexible endoscopic grasping and cutting device and positioning tool assembly. United States patent US 20020103498. 2002 Aug 1

Statistical data

Write as mean ± SD or mean ± SE.

Statistical expression

Express *t* test as *t* (in italics), *F* test as *F* (in italics), chi square test as χ^2 (in Greek), related coefficient as *r* (in italics), degree of freedom as υ (in Greek), sample number as *n* (in italics), and probability as *P* (in italics).

Units

Use SI units. For example: body mass, m (B) = 78 kg; blood pressure, p (B) = 16.2/12.3 kPa; incubation time, t (incubation) = 96 h, blood glucose concentration, c (glucose) 6.4 ± 2.1 mmol/L; blood CEA mass concentration, p (CEA) = 8.6 24.5 μg/L; CO_2 volume fraction, 50 mL/L CO_2, not 5% CO_2; likewise for 40 g/L formaldehyde, not 10% formalin; and mass fraction, 8 ng/g, *etc.* Arabic numerals such as 23, 243, 641 should be read 23 243 641.

The format for how to accurately write common units and quantums can be found at: http://www.wjgnet.com/1949-8470/g_info_20100313185816.htm.

Abbreviations

Standard abbreviations should be defined in the abstract and on first mention in the text. In general, terms should not be abbreviated unless they are used repeatedly and the abbreviation is helpful to the reader. Permissible abbreviations are listed in Units, Symbols and Abbreviations: A Guide for Biological and Medical Editors and Authors (Ed. Baron DN, 1988) published by The Royal Society of Medicine, London. Certain commonly used abbreviations, such as DNA, RNA, HIV, LD50, PCR, HBV, ECG, WBC, RBC, CT, ESR, CSF, IgG, ELISA, PBS, ATP, EDTA, mAb, can be used directly without further explanation.

Italics

Quantities: *t* time or temperature, *c* concentration, *A* area, *l* length, *m* mass, *V* volume.
Genotypes: *gyrA*, *arg* 1, *c myc*, *c fos*, *etc.*
Restriction enzymes: *Eco*RI, *Hin*dI, *Bam*HI, *Kbo* I, *Kpn* I, *etc.*
Biology: *H. pylori*, *E coli*, *etc.*

Examples for paper writing

Editorial: http://www.wjgnet.com/1949-8470/g_info_20100313182341.htm

Frontier: http://www.wjgnet.com/1949-8470/g_info_20100313182448.htm

Topic highlight: http://www.wjgnet.com/1949-8470/g_info_20100313182639.htm

Observation: http://www.wjgnet.com/1949-8470/g_info_20100313182834.htm

Guidelines for basic research: http://www.wjgnet.com/1949-8470/g_info_20100313183057.htm

Guidelines for clinical practice: http://www.wjgnet.com/1949-8470/g_info_20100313183238.htm

Review: http://www.wjgnet.com/1949-8470/g_info_20100313183433.htm

Original articles: http://www.wjgnet.com/1949-8470/g_info_20100313183720.htm

Brief articles: http://www.wjgnet.com/1949-8470/g_info_20100313184005.htm

Case report: http://www.wjgnet.com/1949-8470/g_info_20100313184149.htm

Letters to the editor: http://www.wjgnet.com/1949-8470/g_info_20100313184410.htm

Book reviews: http://www.wjgnet.com/1949-8470/g_info_20100313184803.htm

Guidelines: http://www.wjgnet.com/1949-8470/g_info_20100313185047.htm

SUBMISSION OF THE REVISED MANUSCRIPTS AFTER ACCEPTED

Please revise your article according to the revision policies of *WJR*. The revised version including manuscript and high-resolution image figures (if any) should be re-submitted or uploaded online. The author should send copyright transfer letter, and responses to the reviewers and science news to us *via* email.

Editorial Office

World Journal of Radiology

Editorial Department: Room 903, Building D,
Ocean International Center, No. 62 Dongsihuan Zhonglu,
Chaoyang District, Beijing 100025, China
E-mail: wjr@wjgnet.com
http://www.wjgnet.com
Telephone: +86-10-8538-1892
Fax: +86-10-8538-1893

Language evaluation

The language of a manuscript will be graded before it is sent for revision. (1) Grade A: priority publishing; (2) Grade B: minor language polishing; (3) Grade C: a great deal of language polishing needed; and (4) Grade D: rejected. Revised articles should reach Grade A or B.

Copyright assignment form

Please download a Copyright assignment form from http://www.wjgnet.com/1949-8470/g_info_20100313185522.htm.

Responses to reviewers

Please revise your article according to the comments/suggestions provided by the reviewers. The format for responses to the reviewers' comments can be found at: http://www.wjgnet.com/1949-8470/g_info_20100313185358.htm.

Proof of financial support

For paper supported by a foundation, authors should provide a copy of the document and serial number of the foundation.

Links to documents related to the manuscript

WJR will be initiating a platform to promote dynamic interactions between the editors, peer reviewers, readers and authors. After a manuscript is published online, links to the PDF version of the submitted manuscript, the peer-reviewers' report and the revised manuscript will be put on-line. Readers can make comments on the peer reviewer's report, authors' responses to peer reviewers, and the revised manuscript. We hope that authors will benefit from this feedback and be able to revise the manuscript accordingly in a timely manner.

Science news releases

Authors of accepted manuscripts are suggested to write a science news item to promote their articles. The news will be released rapidly at EurekAlert/AAAS (http://www.eurekalert.org). The title for news items should be less than 90 characters; the summary should be less than 75 words; and main body less than 500 words. Science news items should be lawful, ethical, and strictly based on your original content with an attractive title and interesting pictures.

Publication fee

WJR is an international, peer-reviewed, Open-Access, online journal. Articles published by this journal are distributed under the terms of the Creative Commons Attribution Non-commercial License, which permits use, distribution, and reproduction in any medium, provided the original work is properly cited, the use is non commercial and is otherwise in compliance with the license. Authors of accepted articles must pay a publication fee. The related standards are as follows. Publication fee: 1300 USD per article; Reprints fee: 350 USD per 100 reprints, including postage cost. Editorial, topic highlights, book reviews and letters to the editor are published free of charge.